ESA STM-266
September 2001

Assessment of the Reliability of Solder Joints to Ball and Column Grid Array Packages for Space Applications

P.-E. Tegehall
IVF Industrial Research and Development Corporation, Sweden

B. D. Dunn
Materials and Processes Division
Directorate of Technical and Operational Support
European Space Agency

European Space Agency
Agence spatiale européenne

Assessment of the Reliability of Solder Joints to Ball and Column Grid Array Packages for Space Applications, ESA STM-266

Published by ESA Publications Division, Noordwijk, The Netherlands

ISSN: 0379-4067
ISBN: 92-9092-358-X

Price: 20.00 Euro

Contents

Abstract

Ball Grid Array (BGA) packages are a desirable alternative to surface mount devices such as quad flat packs and small outline packages. The area array distribution of interconnections results in a tremendous saving in board "real estate" but, due to the leadless feature, the solder joint reliability is a concern.

This study has evaluated the suitability of BGAs in spacecraft electronics from a reliability point of view. It consists of a general part and an experimental part. The general part describes BGA technology, important parameters for reliable design and assembly, and methods for post-soldering inspection and rework/repair. In the experimental part, reliability verification testing of ceramic array packages with 625 I/Os has been performed per ECSS-Q-70-08A. Means were explored to improve the reliability such as replacing the balls with columns (Column Grid Array – CGA), restricting the thermal expansion of the PCB (polyimide/aramid), and use of underfill. The fatigue mechanism of solder joints to ceramic BGAs by thermal cycling was investigated using cross-sectioning and dye penetrant analysis. The latter method, originally developed by Motorola, was improved within this study; it is described as an Annex and its ease of use is demonstrated in a case study.

The joints to ceramic BGAs soldered to polyimide/glass PCBs were severely deformed and extensive cracking occurred during thermal cycling. Open joints were registered for some packages before 500 cycles. Application of silicone and epoxy materials as underfill had no significant effect on the fatigue life of the solder joints whereas a significant improvement in fatigue life was obtained for packages with columns instead of balls. Although the fatigue life of the CGA packages with 625 I/Os was improved by a factor of at least two, they still failed the European Space Agency's verification requirement. However, smaller packages are expected to satisfy these environmental test requirements.

A considerable enhancement in fatigue life was obtained both for ceramic BGAs and CGAs when they were soldered to PCBs with very low in-plane thermal expansion (polyimide/aramid). No deformation occurred for the solder joints to the BGAs, but cracks developed in the solder joints predominantly towards the package pads. The improvement in fatigue life of ceramic BGAs soldered to polyimide/aramid compared to polyimide/glass is probably in the order of a factor of four. Nevertheless, even when mounted on polyimide/aramid, the ceramic BGAs failed the verification, but they are on the borderline to pass. Hence, smaller packages are likely to pass the requirement.

The only combination of package and PCB that passed the verification requirement was ceramic CGAs soldered to polyimide/aramid boards. The solder joints to these packages did not show any degradation even after 1000 cycles.

Besides solder joint cracking, cracking was also observed in the laminate beneath solder pads to ceramic BGAs, both on polyimide/glass and polyimide/aramid boards. Cracks in the laminate will in fact enhance the fatigue life of the solder joints, but they may promote other failure mechanisms. If the connection to the pads is achieved using via-in-pads, the copper barrel in the vias may crack resulting in open joints.

1 Introduction

Ball Grid Array (BGA) packages have in a short time become a common component type in consumer products, but also in high-performance products due to their advantageous properties compared to packages with peripheral interconnections [1]. The majority of European Space Agency (ESA) contractors engaged in the design and assembly of spacecraft

electronics have expressed a desire to utilize BGA technology in their circuits, which comprise of multilayer printed circuit boards (PCBs) having at least 14 layers. The main advantages of BGA packages are higher density of I/O interconnections, better thermal and electrical performance, and higher yield in assembly processes. Disadvantages are routing problems due to higher packaging densities, impossibility to visually inspect solder joints, difficulties in repairing/reworking assemblies, and higher cost [2]. Due to the leadless feature and the fact that new technologies are often utilised for production of BGAs, the reliability of the packages is a concern.

It is misleading to talk about BGAs as a homogenous group of packages with similar characteristics. There are numerous types of BGAs [1, 3] and two BGAs of different types may have much more disparate properties when compared with leaded components of different types, e. g. a plastic leaded chip carrier (PLCC) and a leaded quad flat pack (QFP). Except for the form of the leads, leaded components have basically the same build-up and properties. Therefore, it is important to have knowledge of the various types of BGAs and factors affecting their reliability. Since the BGA packages do not have leads, the solder joints are much more vulnerable to fatigue than for leaded components. This, in combination with the inspection and rework/repair difficulties, makes it necessary to understand the important parameters that are required for a reliable assembly process.

The main objectives of this present investigation are to evaluate the reliability and the suitability of BGAs for spacecraft electronics. This work consists of a general part and an experimental part. The general part describes BGA technology, important parameters for reliable design and assembly, and methods for post-soldering inspection and rework/repair. The experimental part focuses on some important parameters for reliable assembly and reliability testing of BGAs and CGAs. Another important objective is to evaluate and demonstrate the "destructive dye penetrant" method that has been developed to quantify the extent of thermal fatigue cracking within grid array solder joints which have been subjected to environmental testing.

2 Description of Ball Grid Array Technology

Most BGA package types are non-hermetic and therefore usually not considered suitable for space applications. There are a limited number of hermetic ceramic BGAs, but the demand for ceramic packages is small since they are considerably more expensive. Also, solder joint reliability is a big concern for ceramic packages if organic printed-circuit boards are used due to the large mismatch in CTEs (Coefficients of Thermal Expansion). Some boards might expand two or three times as much as the ceramic BGA package.

The present trend towards higher performance, smallness, and light weight has resulted in an increasing demand for smaller components and/or higher pin counts. The Quad Flat Pack (QFP) and the Ball Grid Array (BGA) packages today both offer a large number of I/Os, as required by modern integrated-circuit technology. In order to accommodate the increasing number of I/Os needed, the peripheral QFP technology is forced to an ever finer lead pitch with thinner and more fragile leads. The BGA, taking advantage of the area under the package for the solder sphere interconnections, satisfies the I/O demand by using a far coarser pitch (Fig. 1). Additionally, package size and board real-estate required are usually smaller for BGA packages.

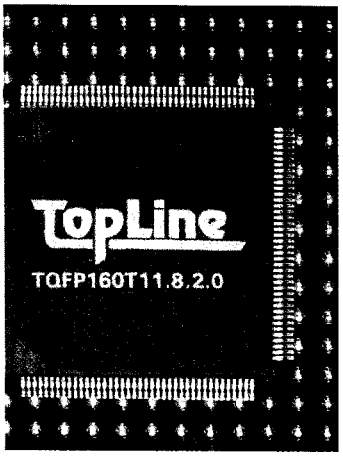

Figure 1. Comparison of a QFP with 160 I/Os (pitch 0.3 mm) placed on top of a BGA with 225 I/Os (pitch 1.5 mm)

The relationship between BGA and QFP package sizes and I/O count is illustrated in Figure 2. A typical 0.65 mm (25.6 mil) fine-pitch QFP with 160 leads measures 28 mm x 28 mm. Modern portable electronics asking for the same number of leads in a package 14 mm x 14 mm ends up at a pitch of 0.3 mm (11.8 mil) with a space between the leads of only 0.15 mm (6 mils). Alternatively, increasing the number of I/Os while retaining the 0.65 mm pitch means a marked increase in package size, e.g. 232 leads in a 40 mm x 40 mm body. A 27 mm x 27 mm plastic BGA (PBGA) houses 225 I/Os with a coarse 1.5 mm pitch. The distance between adjacent solder spheres is approximately 0.8 mm. The more I/Os needed, one is better off with the BGA in terms of package size, since the dimensions only grow as the square root of the I/O count for a given pitch, and not linearly as is the case for QFPs. Around 250 I/Os is believed to be the practical limit for being able to successfully assemble QFPs and, consequently, for I/O counts of over 300, BGAs will have better processing performance and will be more cost efficient when compared to QFPs [4].

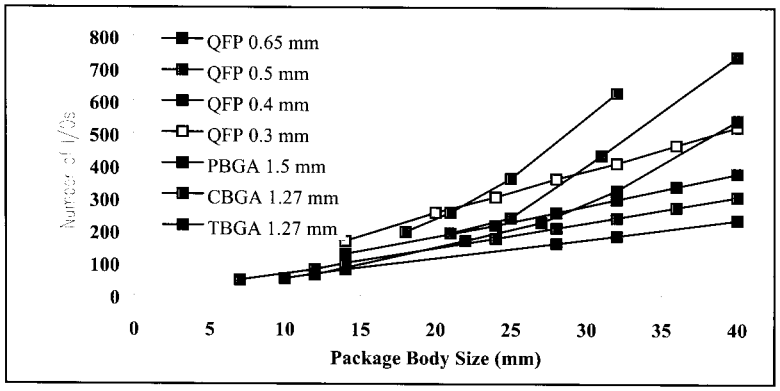

Figure 2. Relationship between BGA and QFP package sizes and I/O counts

In addition, BGA packages afford a more robust construction that is less prone to handling damage. They also provide improved electrical and thermal performance. Spacecraft electronics usually operate in a vacuum so that all thermal energy from Joule heating must be dissipated by thermal conduction, rather than by thermal convection as for terrestrial electronics. Here, BGA packages are far more effective than fine-pitch devices because there is a direct path between the package and its underlying circuit board. The large solder balls have a far better thermal conductivity than that of fine pitch leads which extend from conventional packages.

2.1 Survey of BGA Package Types

Ball grid array packages can be seen as a development of the pin grid array package where the pins have been replaced with solder balls. The first BGAs were ceramic packages developed by Bell Laboratories in 1979-1980 [5]. In 1989, Motorola and Citizen jointly developed the plastic BGA (PBGA). Widespread use of PBGAs was seen in the mid-nineties by, for example, Compaq Computers and Motorola. Since the introduction of the OMPAC (Over Molded Pad Array Carrier), as the PBGA first was known, there have been a tremendous number of new versions or alterations to the original BGA ideas by the very many players in the market. One trend has been to decrease the size of the packages even down to the size of the chip, the ultimate size reduction. Although these packages by definition are BGAs, packages with sizes not more than 20% larger than the chip are generally referred to as Chip Scale Packages (CSPs). This type of package will not be dealt with in this report. However, there is no clear distinction between BGAs and CSPs, since one size of package type may fall within the definition of CSP whereas another size may not. Even packages of the same size but with a different chip size may be classified as different packages types.

Some BGA package types have found widespread use, whereas others have only been produced as prototypes. In this section, the more well-documented package types will be presented. In contrast to conventional component types such as Small Outline (SO), Plastic Leaded Chip Carrier (PLCC), and Quad Flat Pack (QFP), the ball grid array type comprises packages with very heterogeneous construction. Four main categories of BGAs have been identified based on typical characteristics: ceramic packages (CBGAs), plastic packages (PBGAs), tape packages (TBGAs), and metallic packages (MBGAs). However, there is not always a clear distinction between the three latter categories. Therefore, in this report packages will be categorised based on the type of carrier on which the chip is mounted and whether the chip is facing up or down (often referred to as cavity-up and cavity-down packages, although the chip is not always located in a cavity; see Fig. 3).

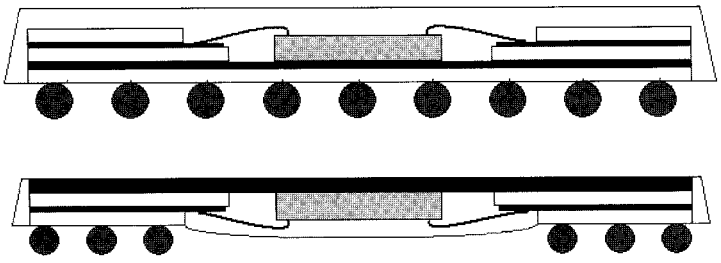

Figure 3. Cavity-up and cavity-down chip mounting

Although early BGAs were ceramic packages, for cost reasons they will mainly be used in products where hermetic packages are required. Consequently, one can expect that there will be a limited number of packages available as ceramic BGAs and these will be comparatively expensive.

The first BGAs had a pitch of 1.5 mm. As the number of I/Os has increased, packages with pitches of 1.27 and 1.0 and even 0.8 mm have become common. Even smaller pitches are used for CSPs.

Ceramic Carriers and Chip Up

The schematic build-up of ceramic packages is shown in Figure 4 [6]. Ceramic BGA packages use cofired multilayer or pressed ceramic substrates [1, 3, 7]. All types of chip interconnection can be utilised (wire bond, flip chip, and TAB). The chip can be protected using a variety of lid sealing or encapsulation techniques. Solder balls usually consist of 10/90 Sn/Pb solder with a melting temperature of about 300°C. Ceramic grid array packages are also available with the solder balls replaced by columns of 10/90 Sn/Pb solder with a height of 1.27 to 2.2 mm [3, 6]. Both balls and columns are usually attached to the package using eutectic solder. Solder columns may also be soldered directly to the package pads.

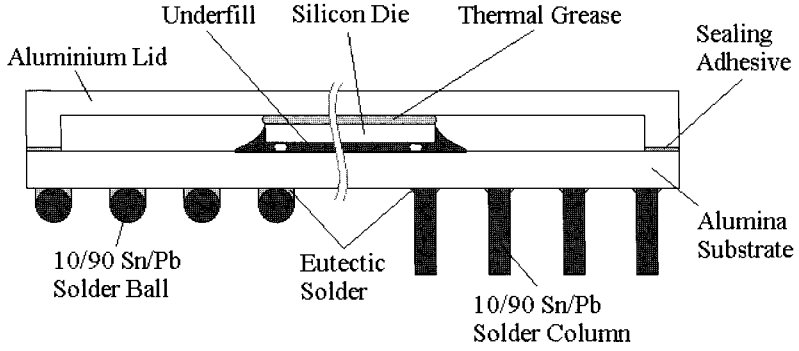

Figure 4. Schematic cross-section of a ceramic solder-grid-array with solder balls and columns

A variation of this package type is the Dimple Ball Grid Array (DBGA). The pads on this package are located in 0.2 mm deep depressions (dimples) in the ceramic substrate [8]. The dimples are filled with Pb/Sn/Bi solder and balls are formed above the dimples (Fig. 5). The solder composition and dimple have been optimised for reliability.

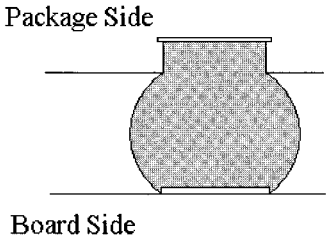

Figure 5. Schematic cross-section of a solder joint to a DBGA

Organic Carriers and Chip Up

BGAs using organic carriers have been developed in a large number of variations. The main characteristics of these plastic BGAs are illustrated in Figure 6, although there are wide variations. A double-sided or multilayer organic substrate is the base in the package. Bismaleimide-triazine (BT) is the most common substrate, but FR-4 and flex films are also used. The chip is usually attached to a metal surface on the substrate using a die attach adhesive. The chip is then wire-bonded to the substrate. The wire bonds and the chip are protected by an epoxy overmold. Alternatively, flip-chip technology may be used to connect the chip to the substrate. Solder balls are reflow-soldered to solder lands on the substrate. Eutectic solder balls are most commonly used. The metallisation of the solder lands usually is autocatalytic nickel/immersion gold. Two alternative methods for definition of the solder lands are available: Solder Mask Defined (SMD) and Non-Solder Mask Defined (NSMD). By

using SMD, the area of the land can be increased without increasing the solderable area, giving a better adhesion of the land to the substrate.

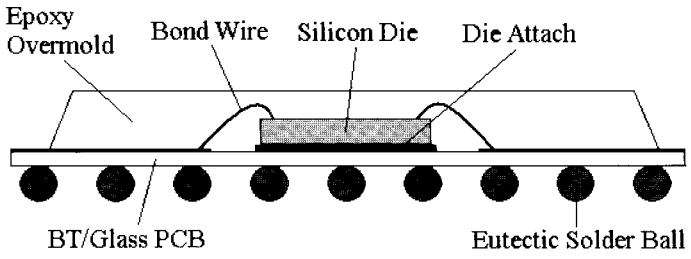

Figure 6. Schematic cross-section of a plastic BGA

Motorola has developed a version with flip chip technology called Flip Chip Plastic BGA (FC PBGA) [9]. The organic substrate is either standard FR4 (or similar) or deposited dielectric board substrate. An underfill is applied beneath the chip to improve reliability. Either eutectic or 10/90 Sn/Pb solder can be used for the solder balls. The package can also be produced as chip down.

IBM's Tape Ball Grid Array package (TBGA) is another representative of this group. In this package, the chip is attached to a polyimide film with copper metallisation on each side using flip chip or TAB technology (Fig. 7)). The tape is adhesively bonded to a copper stiffener plate to provide mechanical rigidity to the package. An optional coverplate over the chip is available for enhanced thermal performance, which then gives the package basically the same characteristics as packages with metal carriers (see below). High melting point solder balls (10/90 Sn/Pb) are used, brazed to via pads on the polyimide substrate [3].

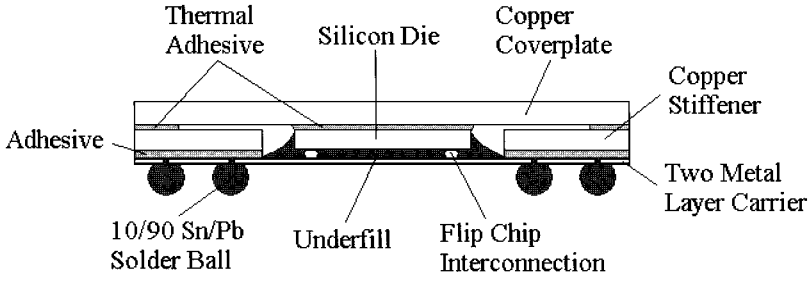

Figure 7. Schematic cross-section of a TBGA

Metal Carriers and Chip Down

A package with the chip mounted on a metal carrier is shown in Figure 8. The die is attached to a metal substrate, usually copper or aluminium. The chip is wire-bonded to a thin film or a laminate. A "glob top" encapsulant is used to protect the chip.

There are numerous types of BGA versions constructed using this technology. One of the most well-known is a package called SuperBGA (SBGA) developed by Amkor/Anam. In this package, the chip is wire-bonded to a thin BT substrate with 1 or 2 metal layers [10]. The BT substrate is attached to a heat-coupling copper ring. Both the copper ring and the chip are attached to a copper heat sink. The upper side of the heat sink is electroplated nickel. In the standard version, there is signal distribution in the BT laminate without power or ground planes, but it is also available in an enhanced version with added power and ground planes. The solder balls consist of eutectic solder (63/37 Sn/Pb).

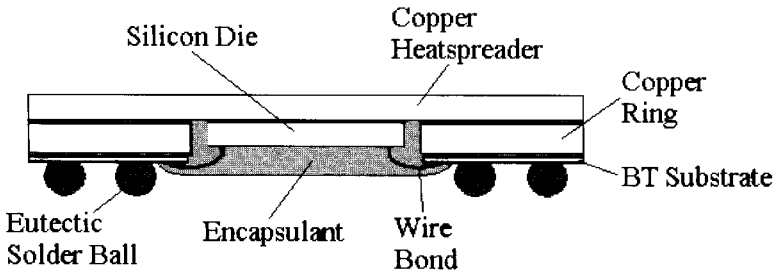

Figure 8. Schematic cross-section of an SBGA

2.2 Reliability of BGAs

The two major failure modes of BGAs are fatigue of solder joints and delamination inside packages. They are affected by a large number of factors, which will be discussed. Some other failure modes will also be described.

Fatigue of Solder Joints

Since BGA packages are leadless, the solder joints are prone to fatigue damage. The main cause of fatigue is the CTE mismatch between package and printed-circuit board (global mismatch). Ceramic packages mounted on organic PCBs are especially likely to fatigue due to the large difference in CTE for ceramic materials and organic PCBs, a mismatch of 10-14 ppm/°C. The thicker the ceramic package's substrate, the shorter the fatigue life [11]. Reliability can be improved by restricting the CTE of the PCB with, for example, a copper-invar-copper layer or by using a ceramic PCB. Fatigue may also be caused by a local expansion mismatch between the solder and the base material of the component or PCB. For ceramic components, this mismatch is about 18 ppm/°C.

Next to ceramic packages, packages with organic carrier and chip up are the most prone to fatigue. This is the result of the silicon die constraining the package's CTE in the region of the die [12]. Thus, the solder joints along the perimeter of the die in the array will experience the highest amount of strain during thermal excursions, and will be the first solder joints to fail. This can be prevented by avoiding the placement of solder balls on the surface beneath the chip (perimeter array) [13]. Consequently, packages with chip down are less inclined to fatigue since solder balls cannot be located on the area occupied by the chip. Also, if the chip is mounted on a metal substrate, the low CTE of the chip will not affect the CTE of the area where the solder balls are located. The reliability of packages with organic substrate and chip up can be improved by decreasing the influence of the chip on the substrate CTE [12-14]. This can be done by increasing the substrate thickness, decreasing the chip thickness, using a thicker die attach or a die attach with lower Young's modulus. The size of the chip will also be important since a smaller chip will affect the CTE on a smaller area.

Beside CTE mismatch, package size has a large influence on expected fatigue life. The larger distance from the neutral point (NP) of a solder joint, the more stress it will be exposed to. Furthermore, the solder land configuration and metallisation have been found to impact the reliability of solder joints. Solder lands with small diameters result in increased package stand-off, which is beneficial from a reliability standpoint. On the other hand, decreased cross-sectional area shortens the time for a crack to result in an open joint [14]. Thus, solder-ball and solder-land sizes need to be carefully optimised. By using solder columns with a high melting point, the stand-off can be increased without decreasing the solderable area. So far, it has only been used for ceramic packages. Fatigue-life improvements of 3 to 10 times have

been reported [6, 15]. Solder composition will also be important. Eutectic solder balls will melt completely and collapse resulting in shorter stand-off, whereas solder balls with high melting point will keep their height [6, 16-18]. The amount of solder added from the solder paste has little impact on the reliability of eutectic solder joints since it only marginally increases the stand-off. In contrast, for balls with a high melting point, the amount of added solder is the most critical feature for maximising the fatigue life of the joint [19]. Too little solder will reduce the diameter of the solder fillet between the ball and the board pad and thereby also the fatigue life, whereas too much solder will cause bridging.

Initial testing of solder balls using a shear test indicated that the weak point was the adhesion of the copper foil to the substrate in the package. The solder ball including the copper foil was ripped off. Therefore, solder mask defined pads were used on the packages, i.e. the solder mask defined the solderable area enabling an increase of the pad diameter without increasing the solderable area. However, actual reliability testing (thermal cycling) has shown that solder mask defined pads give inferior fatigue life compared to non-solder mask defined pads [20, 21]. Both package and printed-circuit board must have non-solder mask defined pads. If only the PCB has non-solder mask defined pads, this will cause increased stress concentration on the package side and somewhat shorter time to failure compared to when solder masked defined pads are used on both sides.

The metallisation of solder lands affects fatigue properties, but somewhat contradicting results have been obtained. Investigations of this subject indicate that organic solderability preservatives (OSPs) give better fatigue life than Ni/Au platings [22]. Nickel/gold and nickel/palladium finishes have been reported to promote cracking [23]. It has been proposed that this is due to enrichment of nickel phosphide in the intermetallic layer [24] or the fact that nickel-tin intermetallic phases are weaker or more brittle than copper-tin intermetallic phases [25]. In the case of nickel/palladium finishes, it may also be due to formation of palladium-tin intermetallic particles [26]. A recent study indicates that the quality problems with Ni/Au platings are traceable to break-down of additives in the nickel bath [27].

The construction of packages with organic carrier and chip up make these packages prone to warpage [2, 16], but other packages may also suffer from it to some extent. Warpage will affect the shape of the solder joints and thereby the fatigue properties. Minor pop-corning may also have this effect [28]

The inclination to fatigue is usually evaluated using thermal-cycling tests. Package and PCB will then have approximately the same temperature. For many products, heating is due to power dissipation. This will result in large temperature gradients inside packages, between packages and PCB, and within the PCB. This is a rather different situation compared to thermal cycling. Even if all materials have matched CTEs, power dissipation may cause fatigue. It has been shown that power cycling and thermal cycling show significant differences in failure location [29]. Therefore, thermal cycling may give misleading results if heating is due to power dissipation. In such cases, power cycling is more appropriate [14, 30].

Because of the leadless feature, BGA technology may not be suitable in cases where long product life, extreme temperature and mechanical conditions, use of large packages, or ultra reliability are required [6, 31]. For these situations, column grid arrays may be an appropriate solution.

Delamination Inside Packages

The polymeric materials used for producing plastic components absorb humidity. Rapid heating of the components, such as during a soldering process, may create a very high water vapour pressure inside the components, causing delamination between different materials or

cracking of materials [32]. The steeper the temperature ramp, the larger the delamination damage [33]. This process is often referred to as "pop-corning". It may occur for all types of plastic components including the traditional standard QFP and PLCC type components.

To avoid pop-corning, plastic components must be stored in dry conditions or be baked prior to a soldering process. Due to material and process optimisation, the inclination for pop-corning of standard components has been reduced although not eliminated. BGA packages are often produced using new materials and manufacturing processes. This has caused many types of BGAs to have a very high inclination for pop-corning damage, especially plastic packages where the chip is mounted on an organic carrier [34]. Packages using ceramic or metallic carriers have less material that can absorb humidity and are therefore less prone to pop-corning.

Thus, it is important that packages are handled properly to avoid pop-corning damage. However, it has been reported that plastic components may have delamination damages in the "as-received" condition from the manufacturer [34, 35]. If that is the case, even following recommended procedures may cause unacceptable damage.

Severe pop-corning may rip off bond wires, cause cracking of the chip, or even open up the package. Minor pop-corning may not cause immediate failure, but it may threaten the long-term reliability due to damaged bond wires and increased risk of bond-wire corrosion and chip metallisation. The activated solder flux used during component assembly is known to have penetrated plastic packages that contained microcracks caused by minor pop-corning. The long-term presence of flux in the vicinity of bonded microwires has resulted in the early failure, due to bimetallic corrosion, of spacecraft flight hardware.

Impact of PCB Properties

Printed circuit boards often have via holes located beneath BGA packages. These holes will have a local effect on the CTE resulting in higher CTE values for the PCB. Perhaps of greater importance, the plating in the via holes will be exposed to large stresses, both during soldering and thermal cycling. In fact, the integrity of the via holes may be affected before any solder joint fails [16]. As BGA pitches decrease and I/O counts increase, the diameters of via holes have to be reduced and at the same time the board thickness increases to accommodate the increased circuitry, causing an increase in the aspect ratio [36]. The higher the aspect ratio (the ratio of PCB thickness and drilled hole diameter), the more difficult it is to plate a copper barrel with good quality inside the via holes. Plating of nickel on top of copper in via holes is said to improve the reliability of the vias [36].

Restricting the CTE in-plane for a PCB by fibres in the x- and y-directions leads to an increased CTE in z-axis. Thus, the more restricted CTE in-plane, the more stressed will be the plating in via holes.

The high interconnection density for BGAs causes routing problems. By using via-in-pad, the routing can be facilitated [37]. The vias need to be blind or, preferably, filled with a polymer and over-plated to prevent loss of solder.

3 Important Parameters for Reliable Assembly Processes

The focus in this chapter will be on reliable assembly processes when using ceramic BGAs.

3.1 Design of Board Pad

If the interconnection of board termination pads to inner layers is made through open vias, a "dogbone" design as shown in Figure 9 is recommended [2, 7, 38]. The conductor interconnecting the terminal pads and the vias should have a width of 0.30 mm and not more than one conductor should be connected to each pad since these are high stress points [38].

Solder dams between the termination pads and the vias created by a solder mask are required in order to prevent loss of solder into the vias. If no solder mask is applied to the PCB, loss of solder to vias must be prevented using some other means. The opening in the solder mask should be larger than the pad (non-solder mask defined) in order to prevent high stress points in the eutectic solder due to interference of the solder mask. For ceramic BGAs and CGAs, IBM recommends a pad diameter of 0.72 mm and a solder mask window of 0.85 mm [38, 39].

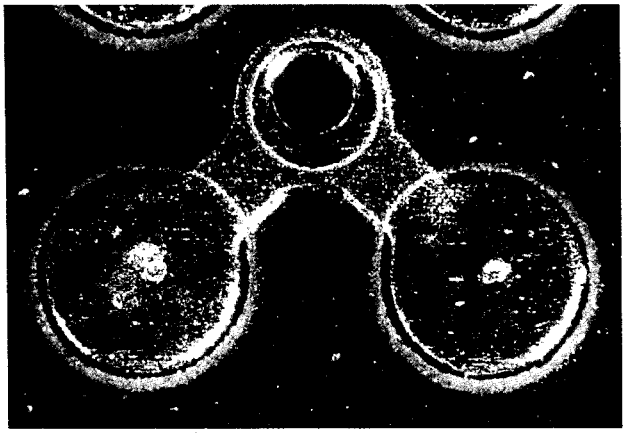

Figure 9. "Dogbone" design of connection between solder pad and via. Two solder pads are connected to the same via in this case

3.2 Printing of Solder Paste

According to Rooks *et al.*, the diameter of the fillet between the ball and the PCB pad is the most critical feature for maximising the fatigue life of ceramic packages with high melt balls [19]. Too little solder paste will increase the risk for opens, but it will also degrade the reliability due to reduced fillet diameter. The diameter should be as large as possible. Therefore, increasing the volume of printed solder paste increases the reliability, but only up to a certain point. When the solder has filled the area between the ball and the board as best it can, extra solder will cause bridging between balls. IBM recommends a minimum fillet diameter of 0.61 mm for a ball with 0.89 mm diameter, and a solder pad diameter of 0.72 mm [38].

Thus, a good print is essential for a reliable assembly process. For ceramic BGAs with 1.27 mm pitch and 0.72 mm PCB pad diameter, IBM recommends a solder volume of 0.10–0.12 mm^3 (6500-7500 $mils^3$) with minimum and maximum volumes of 0.075 and 0.16 mm^3 (4800 and 10000 $mils^3$), respectively [38]. The print height should be not less than 0.18 mm to prevent open joints. A typical good print should have a volume standard deviation not exceeding 7-10%. Apertures with 25 µm taper from top to bottom of the stencil are recommended to facilitate paste release. The aspect ratio (aperture/thickness) should not be less than 3. To ensure that a print is adequate, paste volume measurements should be implemented.

The solder volume requirement usually necessitates that solder paste is printed on the solder mask to some extent, e.g. an aperture of 0.86 mm for a 0.72 mm pad [2, 38]. With good

process control, solder balling will not be a problem. If BGA technology is mixed with fine-pitch technology, it may be necessary to reduce the thickness of the stencil (step down) at the locations of the fine-pitch components.

The diameter of the fillet is not determined just by the amount of solder paste printed on the PCB. Warpage of the package and/or the PCB will also result in reduced fillet diameter. The design of the PCB and the soldering process should be optimised to minimise warpage. Variations in ball diameter may also cause reduced fillet diameter.

Due to the flat bottom of the columns on CCGAs, less solder paste is required for forming a satisfactory joint. A nominal paste volume of 0.078-0.088 mm^3 (5000-5600 $mils^3$) with minimum and maximum volumes of 0.047 and 0.12 mm^3 (3000 and 7600 $mils^3$), respectively, is recommended by IBM [39]. As for CBGAs, the print height should be no less than 0.18 mm to prevent opens. The solder must completely fill under the column and form a fillet that wets at least 180 degrees of the column circumference. Unlike the CBGA package, an increased solder volume will decrease the interconnection reliability of CCGAs since it will increase fillet height and reduce the effective length of the flexible column, making it stiffer.

The final joint of the CCGA has an asymmetrical fillet. This is normal and occurs even if the columns are centred in the paste prior to the reflow and it does not affect the reliability of the solder joints [39].

3.3 Placement

Ceramic BGA and CGA packages are very forgiving during placement. Basically, as long as the solder balls touch solder paste, they will self-align during reflow. The eutectic solder at both the module and PCB will reflow. This allows the high-melt solder ball or column to float and to equilibrate between package and board termination pads.

3.4 Reflow Soldering

The solder reflow profile recommended by the paste supplier should be followed. The peak temperature should not be higher than 220 °C. A higher peak temperature may raise the melting point of the eutectic solder due to dissolution from the high melt ball. It will make rework more difficult, but does not affect the fatigue life [40].

Proper thermal profiling is required to make sure that solder joints beneath the package are properly reflowed. The high thermal mass of ceramic packages may necessitate shielding of some parts of the board to prevent overheating of the laminate and heat-sensitive packages.

3.5 Wave Soldering

If mixed technology including wave soldering is used for manufacturing of assemblies, it may affect the reliability of BGA packages. Filling of vias with molten solder during wave soldering may cause secondary reflow of the BGAs, which in turn can cause cracking of the solder joints. This can be prevented by shielding the via holes with, for example, a polyimide tape or tenting. Warping of the board during wave soldering can also cause cracks in the solder joints to BGAs. Special fixtures or supports may be required to prevent warping. The temperature of BGA solder joints on the topside should not exceed 150°C during wave soldering [2].

4 Methods for Post-Soldering Inspection

Visual inspection of all solder joints to grid array packages is impossible. Thus, good process control is the key to high yields and high reliability. Nevertheless, the outer rows can be inspected and can be used to check for good wetting, fillet size and self-alignment.

Solder joints beneath the package can only be inspected using X-rays. Ball grid arrays with eutectic solder joints can be inspected with transmission systems or laminography systems [41]. By using teardrop pads, open solder joints can be more easily detected. However, this type of system cannot be used to inspect the quality of solder joints with high melt balls because the ball will entirely obscure the eutectic solder fillet in a transmission image [19]. An X-ray system that can be used to inspect these solder joints is Scanned-Beam X-ray Laminography (SBXLAM). This system can focus on a particular horizontal cross-sectional plane and, thereby, isolate the solder fillets from the solder balls, so that open joints can be detected [19]. However, due to laminographic smearing of the solder ball, it is usually not possible to detect solder joints with reduced fillet diameters.

5 Methods for Rework and Repair

Rework and repair are more complicated for grid array packages than for conventional packages because touchup of individual joints is not possible. The whole package must be reworked. Special tooling is needed for this work. A clearance of 5.0 mm around the BGA for rework tooling is required, with the exception of discretes which can be as close as 2.5 mm [38].

IBM recommends the following procedure for rework. A hot-gas reflow tool with a bottom PCB heater is required for removing the package. Preheating between 75 and 125 °C should be performed prior to the application of hot gas from the top heater. This is crucial for minimising PCB warpage and thermal shock. Maximum preheat should be 10 °C below the T_g for the PCB material.

Thermal profiling is essential for package removal. Each CBGA site to be reworked must be individually profiled, due to variations in adjacent packages and the heat-sinking properties of the PCB internal layers. The following points should be monitored: centre and edge joints of the package, adjacent packages, and the PCB.

The hot-gas top heater is used to reflow the solder joints. The joints must be profiled to 190 °C minimum (220 °C maximum) prior to applying vacuum pick-up force. By ensuring that all solder joints are reflowed, lifted PCB pads can be avoided. Adjacent CBGA temperature should be limited to less than 150 °C. If the board is moisture-sensitive or has moisture-sensitive packages, a bake-out for 24 hours at 125 °C prior to rework is required.

Preferably, the flow of hot gas should be directed onto to the top of the package. Deflection of the gas flow underneath the package tends to create non-uniform solder temperature across the array pattern.

After removal of the package, solder balls remaining on the board and as much remaining solder as possible must be removed. The latter has a high lead content and would increase the melting point of new solder paste. Copper dissolution and warping must be minimised during this process.

For soldering a new package to the board, there are several ways to apply the solder, including:

- screen paste onto CBGA package

- screen paste onto PCB site
- solid preforms or decals
- dispense paste onto PCB site.

The same solder volume criteria that apply to initial assembly also apply to rework processes.

The tooling for reflow soldering of the new package is the same as for package removal. The rework thermal profile has the same limitations as in initial assembly. Special attention should be paid to not damage adjacent packages by applying too much heat. A pre-bake may also be required if moisture-sensitive boards and packages are used.

6 Definition of Experimental Work

6.1 Rationale for Choice of Package Type and I/O Count

Ceramic packages are traditionally preferred in space electronics since they are hermetic and are believed to offer better reliability at package level. Today, high-reliability Plastic Encapsulated Microcircuits (PEMs) are available in the form of conventional leaded packages such as Quad Flat Packages (QFPs) and Small Outline Integrated Circuits (SOICs) [42]. The high reliability of PEMs has been achieved by improved encapsulating materials, die passivation, and manufacturing processes. Since plastic BGAs have a quite differing build-up regarding materials and manufacturing processes compared to conventional leaded packages, the long-term reliability of these is uncertain. Therefore, it was decided to choose a ceramic BGA for this investigation despite the better fatigue properties of solder joints to many plastic BGAs.

An I/O count of 625 was chosen since it was anticipated that counts of that order will be requested in the near future.

6.2 Experiment Test Matrix

The experimental work performed in this study consists of two parts. The first part is an evaluation of the fatigue mechanism of solder joints to ceramic BGAs by thermal cycling. Ceramic BGAs have high-lead solder balls that do not melt during the soldering process. The volume of solder paste printed on the solder pad is therefore critical for solder joint reliability. Too little solder paste due to poor print will result in a fillet that has a reduced cross-sectional area between the solder pad and the solder ball with inferior reliability. A reduced cross-sectional area may also be caused by warpage of package and/or board, or by varying solder ball diameters on the package. Therefore, the impact of meagre solder joints on reliability was also studied in this part.

In the second part, reliability verification testing of the packages was performed per ESA PSS-01-738, Chapter 10 [43]. The investigation performed by Jet Propulsion Laboratory [4] indicates that ceramic BGAs will be on the borderline for passing the ESA requirement regarding solder-joint reliability. Therefore, the second part also includes means to improve the reliability of ceramic BGAs. The means that have been evaluated are:

- Use of columns instead of balls on the package (Column Grid Array).
- Use of a printed board with more restricted in-plane CTE.
- Use of conformal coating.
- Use of underfill.

7 Materials

7.1 Packages

Ceramic ball grid array and column grid array packages from IBM were used for the tests. Both types of modules had a 2.0 mm thick ceramic multilayer substrate and an aluminium lid. They had 625 I/Os (25 x 25 full array) with a pitch of 1.27 mm and daisy-chain interconnection (Fig. 10). The body size was 32.3 mm x 32.3 mm. No chip was mounted in the modules.

Both the balls and the columns consisted of high melt solder (10% Sn/90% Pb) and were soldered to the modules using eutectic solder. The balls had a diameter of 0.89 mm whereas the columns had a diameter of 0.51 mm and a height of 2.2 mm (Fig. 11).

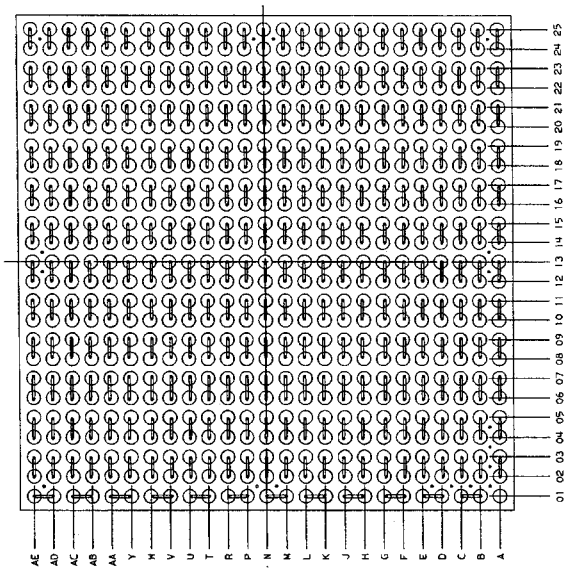

Figure 10. Package daisy chain (bottom view)

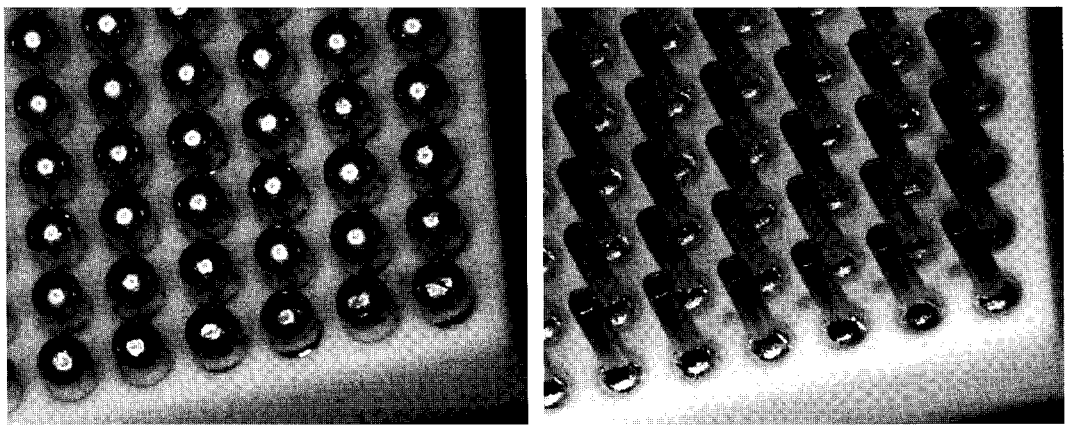

Figure 11. Photographs showing the balls and columns, respectively, on the tested package types. The balls and the columns have diameters of 0.89 mm and 0.51 mm, respectively

7.2 Printed Boards

Four-layer printed boards were manufactured by Printca AS, Denmark, per ESA PSS-01-710 [44]. They were manufactured using two different types of laminates: polyimide/glass and Thermount 85NT. Thermount 85NT is a non-woven aramid reinforced polyimide substrate, which has a very low in-plane CTE of 6-9 ppm/°C. The CTE of printed-circuit boards is usually slightly higher due to the copper content. A typical 12-layer PCB has an in-plane CTE of about 10 ppm/°C.

The printed boards were 233 mm x 160 mm and 2.0 mm thick. Each board was mounted with four packages (Fig. 12). The footprint design shown in Figure 13 was used for both CBGA and CCGA packages. A daisy-chain interconnection was achieved on the board by connecting pairs of solder lands to vias as shown in Figure 9. Thereby, opens in the daisy chain can be localised to pairs of solder joints by probing on the backside of the board. The solder land connection to vias had the "dogbone" design recommended by IBM [38]. The pad and via land diameters were nominally 0.72 mm and 0.61 mm, respectively. The actual pad diameters on the polyimide/glass and the Thermount boards were determined to be 0.70 mm and 0.72 mm, respectively.

In order to prevent loss of solder to the vias during soldering, a solder mask was applied to the boards (SD2467 SM-DG from Lackwerke Peters). The solder mask opening at the pads was 0.85 mm, i.e. larger than the pad diameter (non-solder mask defined pad). The solder mask opening at the via lands was 0.48 mm. Hot-air solder levelling was used as surface finish since use of fused tin/lead is not possible when a solder mask is applied to the board. Holes with a diameter of 2.0 mm were drilled in the boards in order to fix them to a shaker during a vibration test.

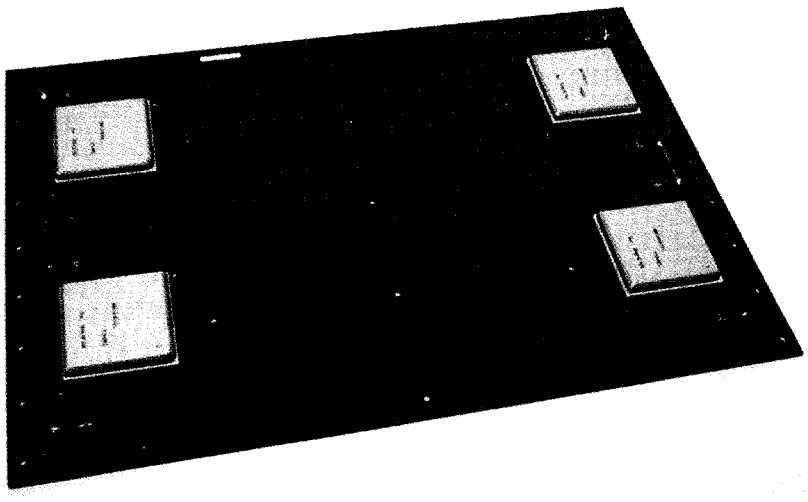

Figure 12. Test vehicle used for the evaluations

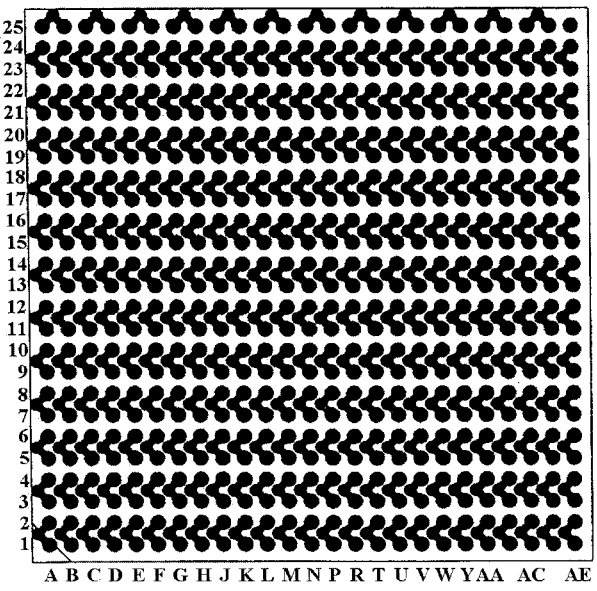

Figure 13. Footprint design for mounting of CBGA and CCGA packages

7.3 Conformal Coating

Spacecraft electronics are usually treated with a conformal coating to protect them prior to launching. Due to the array distribution of the connections to CBGAs and CCGAs, they present a special challenge from a coating point of view. All solder joints must be coated, but application of too much coating material completely filling the space between the package and board may cause increased mechanical stressing of the solder joints leading to a shorter fatigue life. On the other hand, it has been found that especially Parylene and silicone conformal coatings may improve the fatigue life of solder joints to leaded components and leadless ceramic chip carriers (LCCCs) [45, 46].

For these reasons, a solvent-free silicone material, CV4-2500 from NuSil Technology, was chosen to be applied under the packages. CV4-2500 is a two-part, optically clear RTV silicone developed to be used as an embedding or potting compound.

7.4 Underfill

Specially designed underfills have been developed to improve the fatigue life of solder joints to flip chips and CSPs. Their function is to redistribute the mechanical forces on the solder joints so that they are stressed more evenly. They may also improve the shock-proof strength of CSPs and BGAs. The CTE values of the underfills are usually more or less matched to the CTE value of solder (about 25 ppm).

Two epoxy underfills were tested in this investigation, OHMCOAT 1570 and OHMCOAT 1572, from NAMICS Corporation. They have CTE values of about 25 ppm and 60 ppm respectively. The higher CTE of OHMCOAT 1572 is due to a lower filler content. The low filler content decreases the viscosity and thereby facilitates the application of the material.

8 Manufacture of Test Vehicles

For the first part of this investigation, the fatigue mechanism of solder joints, ten test vehicles of BGAs mounted on glass-reinforced polyimide boards were manufactured. Five of the test vehicles were manufactured using a stencil with reduced aperture to achieve "meagre" solder fillets.

The complete test matrix for the second part, reliability verification, is given in Table 1. Two test boards equipped with four packages were manufactured for each combination of laminate, package and underfill material.

Table 1. Test matrix for reliability verification testing of CBGA and CCGA packages per ESA PSS-01-738

Board no.	Printed board	Package type	Underfill material
P1 and P2	Polyimide/glass	CBGA	None
P3 and P4	Polyimide/glass	CBGA	CV4-2500
P5 and P6	Polyimide/glass	CBGA	OHMCOAT 1570
P7 and P8	Polyimide/glass	CCGA	None
P9 and P10	Polyimide/glass	CCGA	CV4-2500
P11*	Polyimide/glass	CCGA	OHMCOAT 1570
T1 and T2	Thermount 85NT	CBGA	None
T3 and T4	Thermount 85NT	CBGA	CV4-2500
T5 and T6	Thermount 85NT	CBGA	OHMCOAT 1572
T7 and T8	Thermount 85NT	CCGA	None
T9 and T10	Thermount 85NT	CCGA	CV4-2500
T11 and T12**	Thermount 85NT	CCGA	OHMCOAT 1572

* There was only enough material to apply under the packages on one board
** Underfill was applied under three of the four packages on Board T12

8.1 Baking of Printed Boards

Delamination may occur in the printed-board laminate if it is not baked prior to soldering. Especially the Thermount laminate have a high inclination for this type of behaviour [47]. Therefore, the printed boards were baked at 125 °C for 4 hours prior to soldering.

8.2 Printing of Solder Paste

An RMA solder paste, Cleanline UP78T (62Sn/36Pb/2Ag) from Alpha Metals, was printed on the test boards using a stainless-steel stencil with a thickness of 200 μm. An aperture of 0.86 mm was used, as recommended by IBM for CBGAs. This gives a print with a solder volume of approximately 0.12 mm^3. The aperture is larger than the pad diameter, i.e. the print will be on the laminate to some extent. This did not cause any problem with solder balling. The same stencil was used for soldering of both CBGAs and CCGAs.

To achieve "meagre" solder fillets on five test boards, a stencil was used with the apertures reduced for six solder joints in each corner of the packages. The intention was to reduce the solder paste volume by 25% and 50% respectively but, by mistake, the aperture was decreased by these figures. That is, for two packages on each board the aperture was reduced by 25% and for the remaining two by 50%. This gave solder volume reductions of 44% and 75% respectively, i.e. solder paste volumes of about 0.068 and 0.030 mm^3, respectively. That compares with the minimum solder paste volume of 0.075 mm^3 recommended by IBM [38].

8.3 Mounting of Packages

The packages were mounted on the boards using a Zevac DRS 24 soldering and desoldering machine.

8.4 Soldering of Packages

An SMT convection oven was used for reflow soldering. The profile used is shown in Figure 14. Examination of the solder joints using microfocus X-ray equipment showed very few voids in the solder connections towards the boards, both for CBGA and CCGA packages.

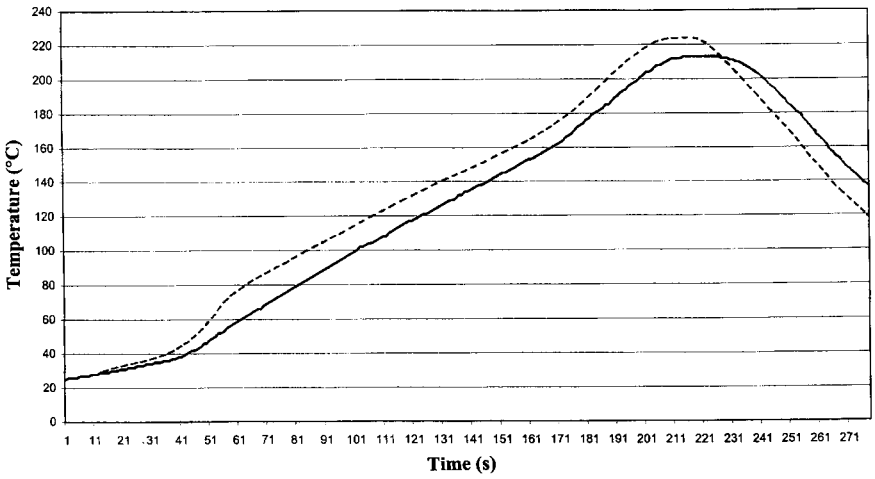

Figure 14. Temperature profile used for soldering of test vehicles measured for CBGA centre joint (unbroken line) and corner joint (broken line)

Figure 15 shows the visual appearance of solder joints to the CBGAs. For most, the solder ball was perfectly centred in the joint. Figure 15 also shows a solder joint with maximum observed tilting of the ball. Cross-sections of solder joints are shown in Figure 16. The solder joints had the same appearance on the polyimide/glass and the Thermount boards.

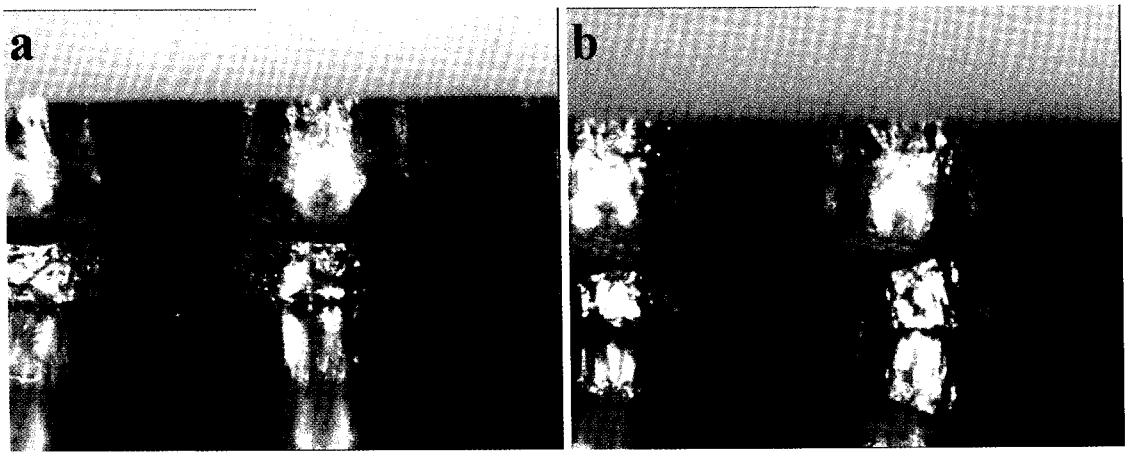

Figure 15. Photographs of solder joints to BGAs showing the spread in ball centring from perfectly centred balls (a) to maximum tilted balls (b)

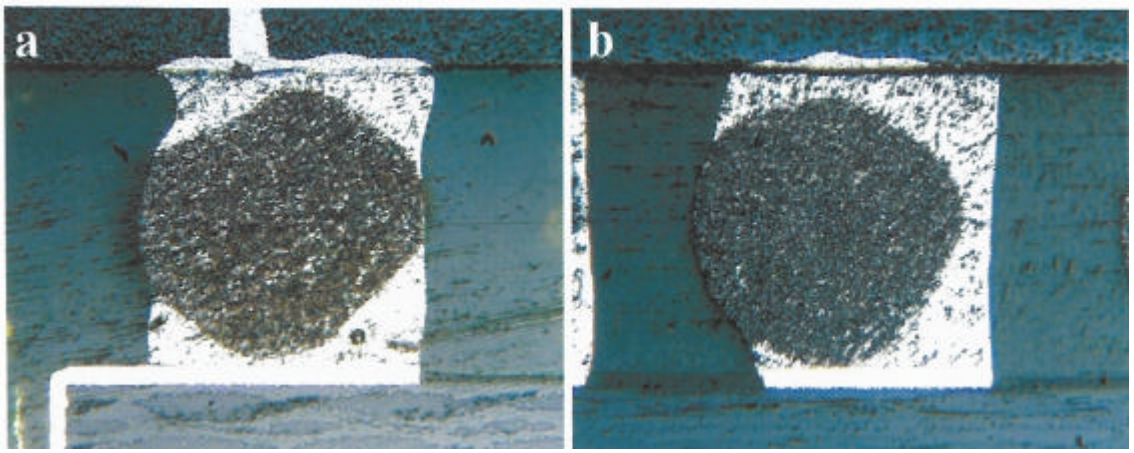

Figure 16. Cross-sections of a perfectly centred ball (a) and a maximum tilted ball (b)

Solder joints formed using reduced amounts of solder paste are shown in Figures 17-19. A 44% reduction in solder paste gave a fillet diameter of about the same size as the pad diameter, i.e. about 0.70 mm, whereas a 75% reduction in the solder paste volume caused a decrease in the solder fillet diameter to 0.55 - *0.60* mm, i.e. a 15% to *20%* reduction.

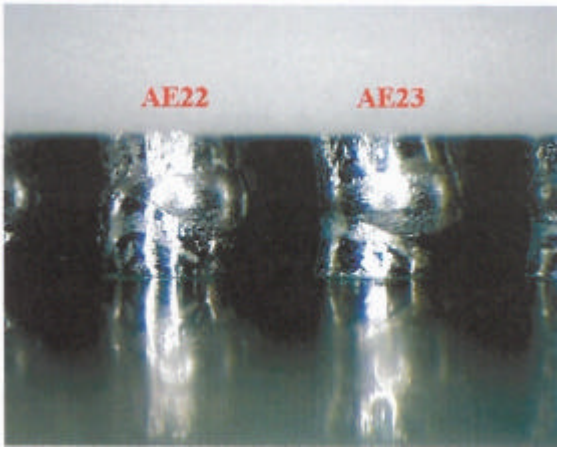

Figure 17. Solder joints to CBGA with solder paste volume reduced by 44% for corner joints, in this case the ball to the right

Figure 18. Solder joints to CBGA with solder paste volume reduced by 75% for corner joints, in this case the ball to the left

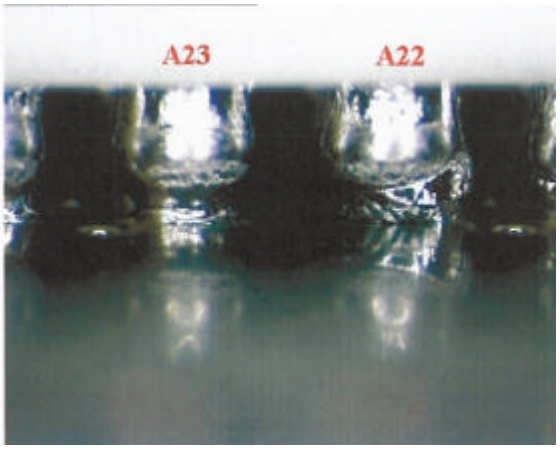

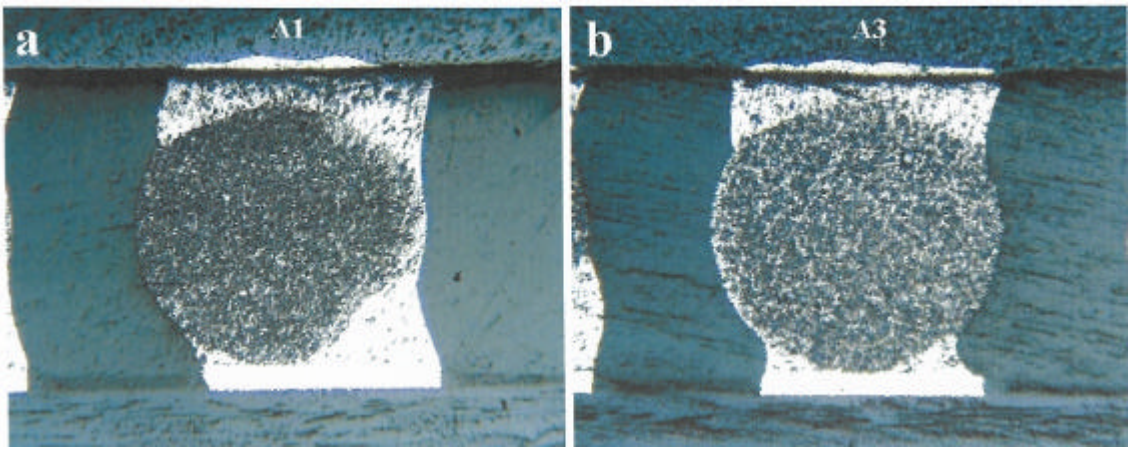

Figure 19. Cross-sections of solder joints formed with reduced solder paste volume, to the left by 44% and to the right by 75%

The columns on the CCGAs were aligned to the edge of the pads on the printed boards, resulting in asymmetrical fillets (Fig. *20)*, which is normal [39]. Most solder joints were tilted in the same direction, but not always (Fig. *21)*.

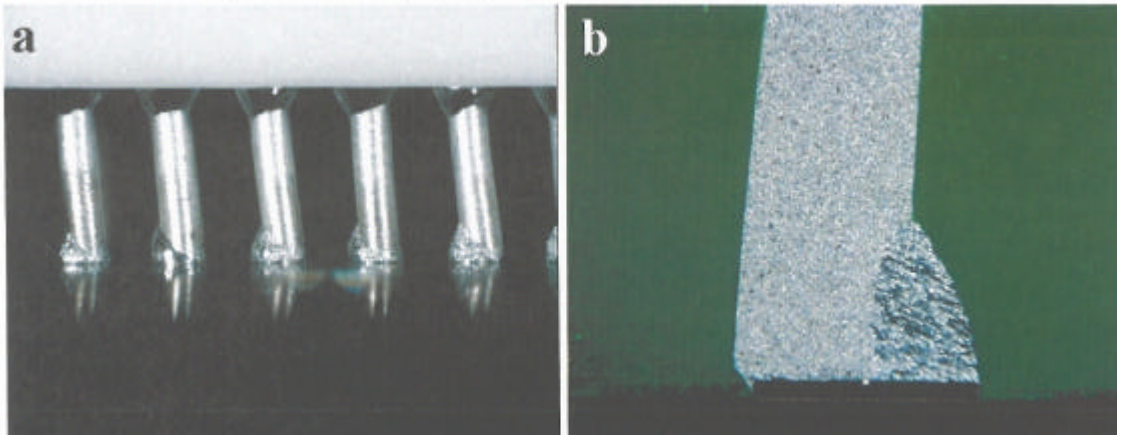

Figure 20. Appearance of solder joints formed to a CCGA

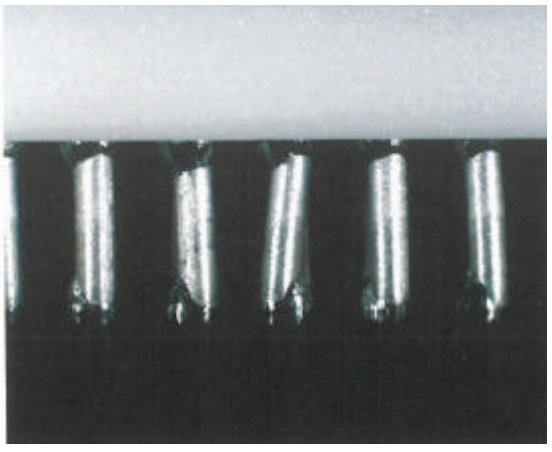

Figure 21. Ceramic CCGA with columns tilted in different directions

8.5 Cleaning

The soldered boards were cleaned in Zestron LP at 50 °C for 10 min using ultrasonic agitation. Zestron LP is a blend of di(propylene glycol) ethyl ether and propylene glycol

dialkyl ether with a boiling point of 160-220 °C. After cleaning, the boards were first washed with isopropanol followed by deionised water, and then once more with isopropanol. Finally, the boards were blown dry with nitrogen and then heated in an oven at 100 °C for 4 hours. Visual inspection of the area beneath a package on a spare board showed that no visible flux residues remained after this cleaning procedure. The package was mechanically removed by bending the board so that the pads on the boards were ripped from the laminate.

8.6 Application of CV4-2500

The CV4-2500 material was applied along one side of the packages at room temperature and was sucked in under them by capillary forces. The application was done manually using a syringe. A polyimide tape was applied over the via holes on the opposite side of the boards to prevent the coating material from escaping through them. Material was added until it become visible at the opposite side of the packages. The polyimide tape was then removed and curing of the CV4-2500 material was performed at 65 °C for 60 min.

8.7 Application of OHMCOAT 1570 and 1572

The underfills were applied using Asymtek DP-2000 dispensing equipment. Both the underfill material and the test board can be heated in this equipment to improve the fluidity of the underfill. When applying OHMCOAT 1570, the underfill and the test board were heated to 50 °C, while when applying OHMCOAT 1572 they were heated to 30 °C. Application was made along one side of the packages (Fig. 22). Material was added until it became visible at the opposite side of the packages. As when applying the conformal coating, polyimide tape was applied over the via holes on the opposite side of the boards. This polyimide tape was then removed and curing was performed at 120 °C for 20 min.

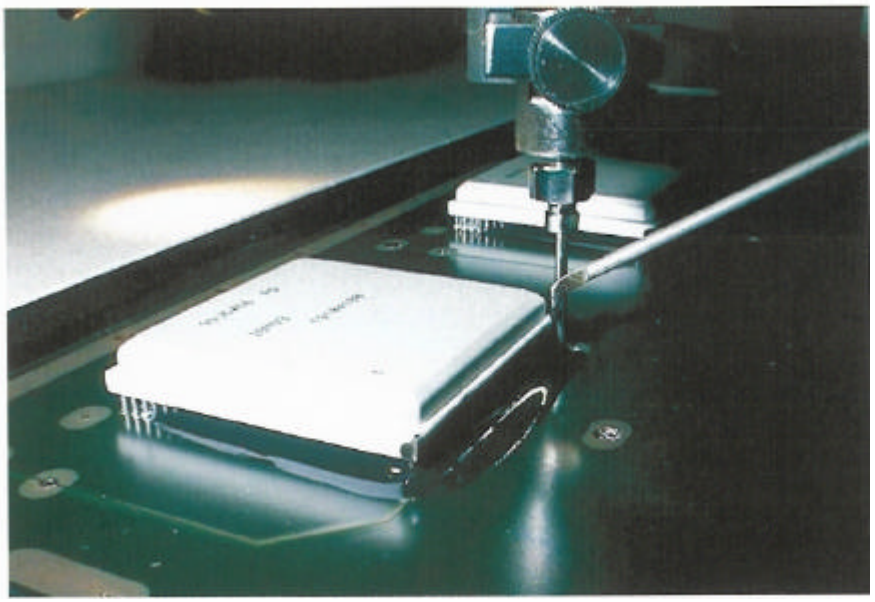

Figure 22. Application of underfill along one side of the packages

9 Reliability Verification Methods

Reliability testing was done by a combined temperature cycling/vibration test. In order to simulate true conditions as much as possible, the test was started with 100 thermal cycles followed by the vibration test and then another 900 thermal cycles. The idea was that vibration testing might have a much larger impact on crack propagation than on crack

initiation. Since testing prior to launching could initiate cracks, the purpose of the first 100 thermal cycles is to simulate such testing.
For the first part, evaluation of fatigue mechanism, the vibration test was not executed.

9.1 Thermal-Cycling Test

Temperature cycling was performed as per ECSS-Q-70-08A, Section 13.2 [48]. An air-circulating oven, Heraeus HT 7015-10/S, was used for the test. The temperature was cycled between -55 and +100 °C with a temperature ramp of 10 °C/min and a soak time of 15 min at each temperature extreme. The actual temperature profile measured for a corner lead to a package is shown in Figure 23.

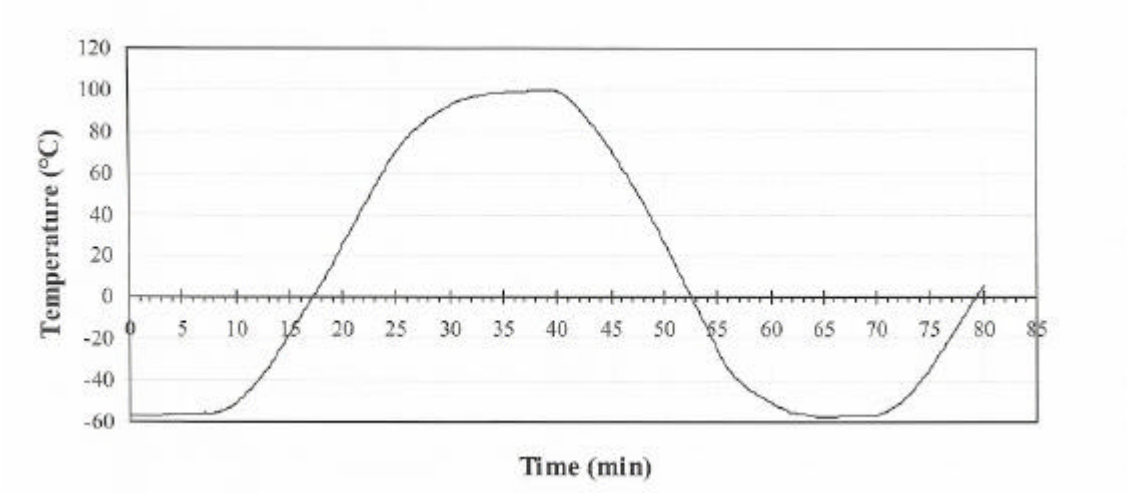

Figure 23. Temperature profile measured for a corner lead to a CBGA during the thermal cycling test

An Anatek 1281VF high-speed event detector was used for monitoring resistance of the daisy chains *in situ* in the temperature-cycling chamber. The event detector records ultrashort spikes or open circuits in the daisy chains, provided the spikes last at least 1 μs. An open circuit was defined in this case as a total daisy-chain resistance above 100 ohms, i.e. about 5 times the measured resistance of the BGA daisy chain prior to the test.

A failure was defined as the first interruption of electrical continuity that is confirmed by 9 additional interruptions within an additional 10% of the cycle life per the recommendation in IPC-SM-785 [49].

Due to a limited number of channels, the packages were connected two by two during the measurements. Connection to the boards was made with wires soldered to the boards.

9.2 Vibration Test

Sine and random vibration testing were performed using the conditions given in Table 2, which reflect the minimum severity for vibration testing given in Chapter 13 of ECSS-Q-70-08A [48]. The vibration testing was performed in two axes, one parallel to the long side of the test board and one perpendicular to the test board.

Table 2. Severity levels used for vibration testing

Sine vibration	Frequency range	10-2000 Hz (CPS) at 15 g
	Vibration amplitude	(Peak to peak) 10-70 Hz at 1.5 mm
	Sweep speed	1 octave per minute
	Duration	1 cycle from 10-2000-10 Hz
Random vibration	Frequency range	20-2000 Hz at 15 g (RMS)
	Power spectral density	0.1 g^2/Hz
	Duration	10 min per axis

The test boards were fixed directly to the vibration board using five steel bars as shown in Figure 24. The screws were drawn with a moment of 0.25 - 0.27 Nm. Four product response accelerometers were attached to the test boards in the positions shown in Figure 24. The registered responses for the board with CBGAs and CV4-2500 as underfill are shown in Figures 25 and 26. The responses were very similar for the other boards.

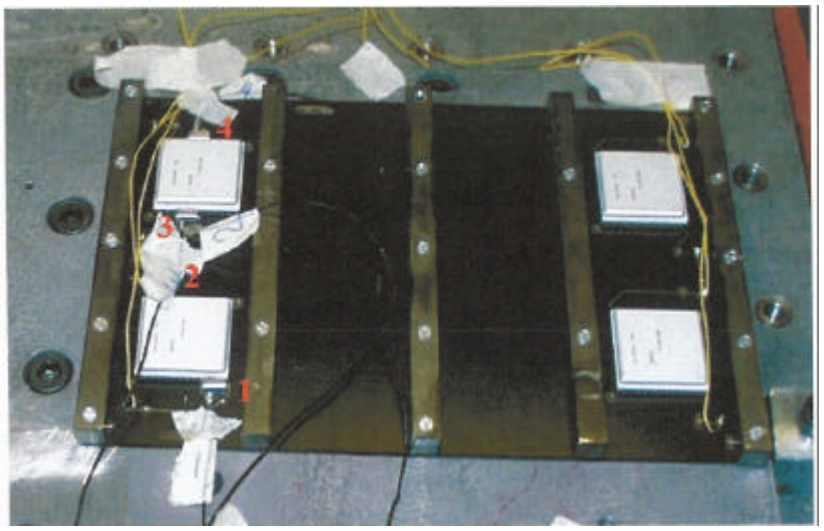

Figure 24. View of test board mounted on the vibration exciter

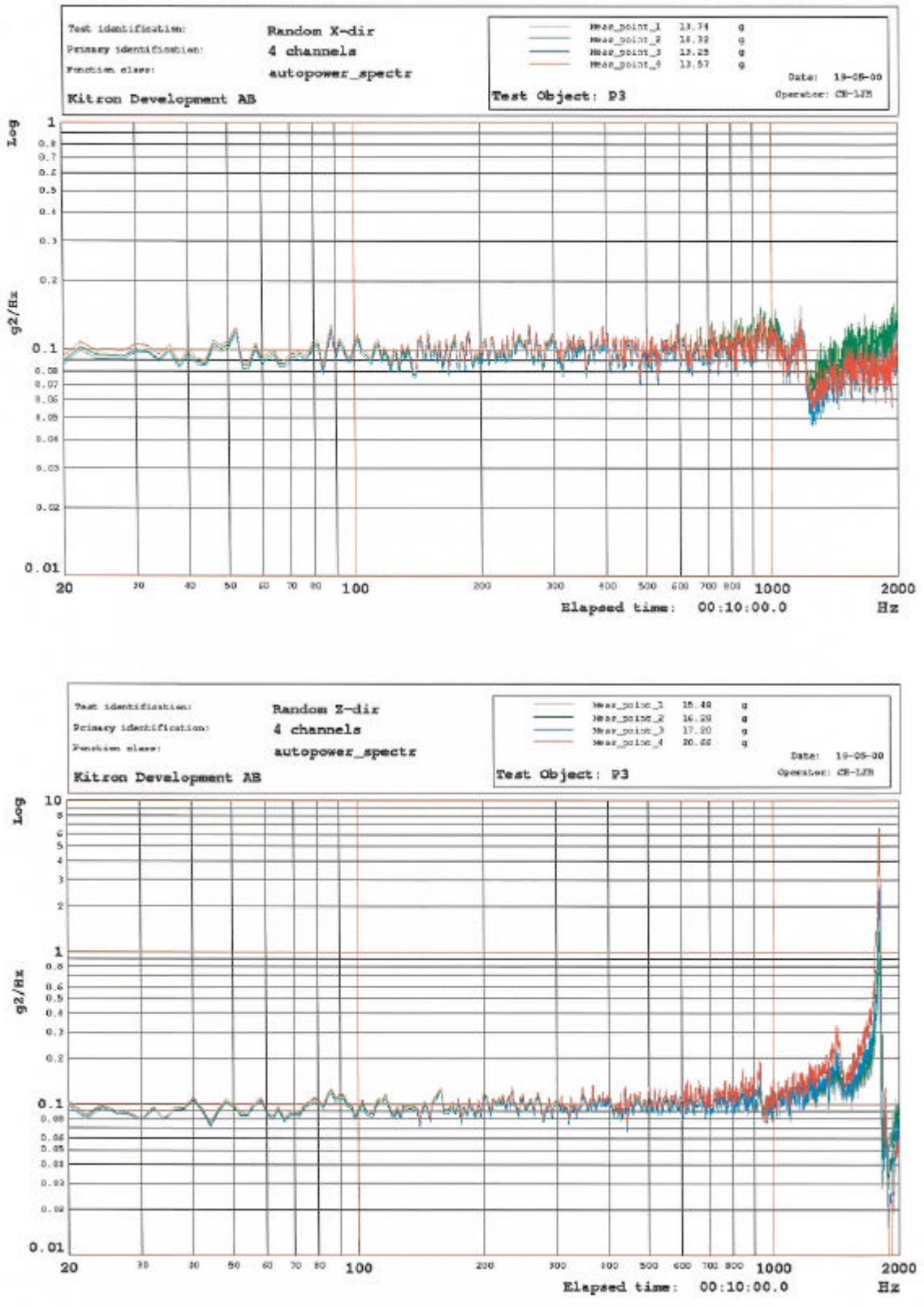

Figure 25. Acceleration spectral density recorded during the random vibration test in the x-direction (upper diagram) and in the z-direction (lower diagram) for the board with CBGAs and CV4-2500 as underfill

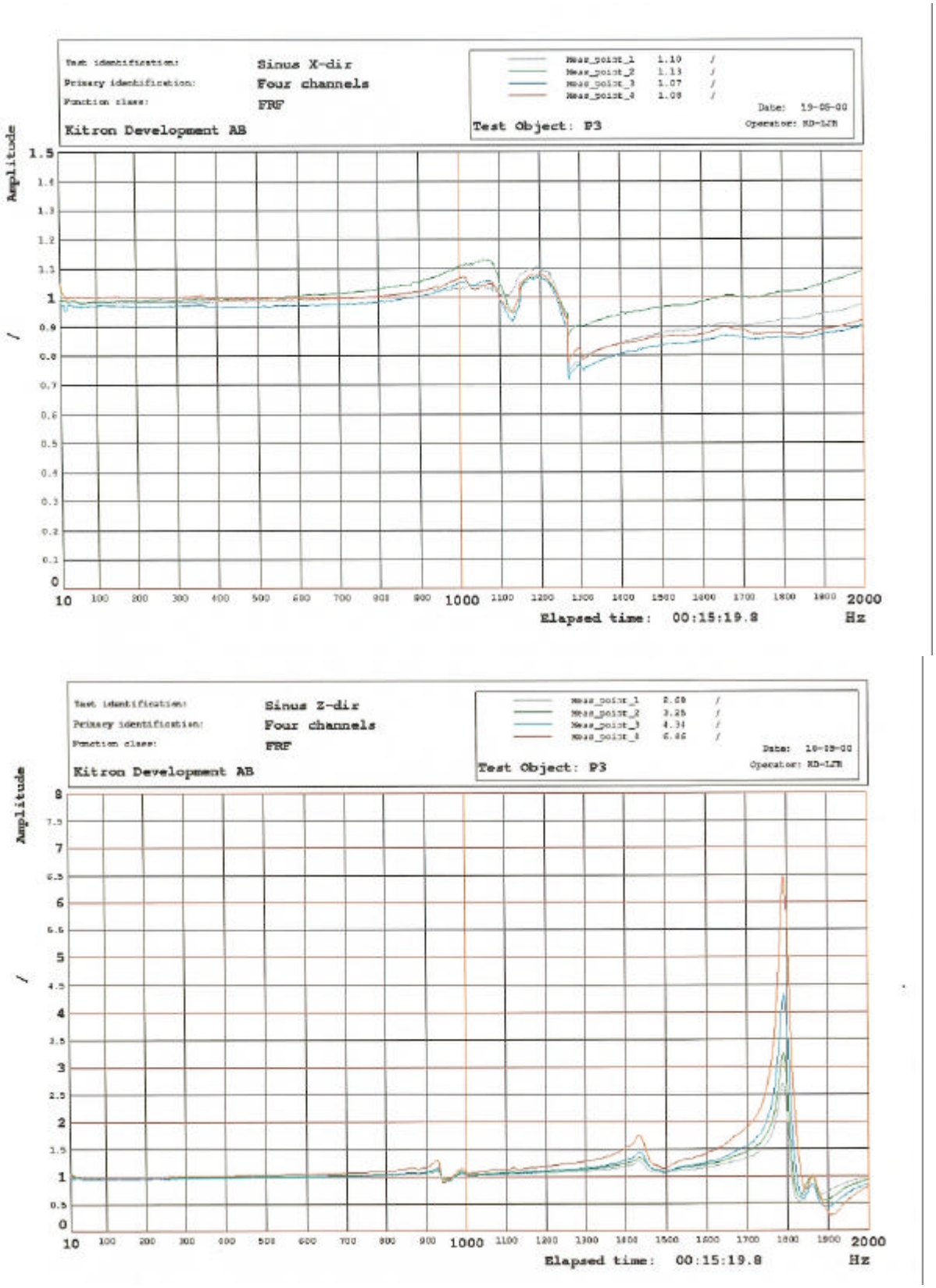

Figure 26. Acceleration recorded during the sine vibration test in the x-direction (upper diagram) and in the z-direction (lower diagram) for the board with CBGAs and CV4-2500 as underfill

9.3 Analysis Methods

After testing, the impact on the integrity of the solder joints was analysed using two techniques. The first technique involves the standard metallurgical practice of cross-sectioning and polishing samples potted in epoxy. An epoxy with an added fluorescent agent was used to facilitate the detection of cracks. The cross-sectioned samples were studied using optical microscopy.

The cross-sectioning technique offers only a planar view of the solder joint. A three-dimensional view of a crack can be obtained by using dye penetrant analysis. Dye penetrant analysis was originally developed by Motorola [12]. In this method, the packages were mechanically removed after the application of the dye through bending the board numerous times. The method works well if the cracks in the solder joints are large. If they are not large enough, the pads on the board are ripped from the laminate. A method of removing the components that allows the solder joints to creep during the removal has been developed in this project and is described in Annex A. It is important to note that by using this method, even small cracks can be detected.

10 Results

10.1 Impact of Thermal Cycling on Solder Joint Reliability

Two test boards with CBGAs on polyimide/glass were cycled until all eight packages had failed. The cycles-to-failure are presented in Figure 27. The packages were connected two by two during the measurements. For two pairs of packages, both packages in each pair had failed before the package failing first was disconnected. Therefore, the exact numbers of cycles-to-failure for failures 4 and 6 are not known, but they occurred between cycle 725 and cycle 816.

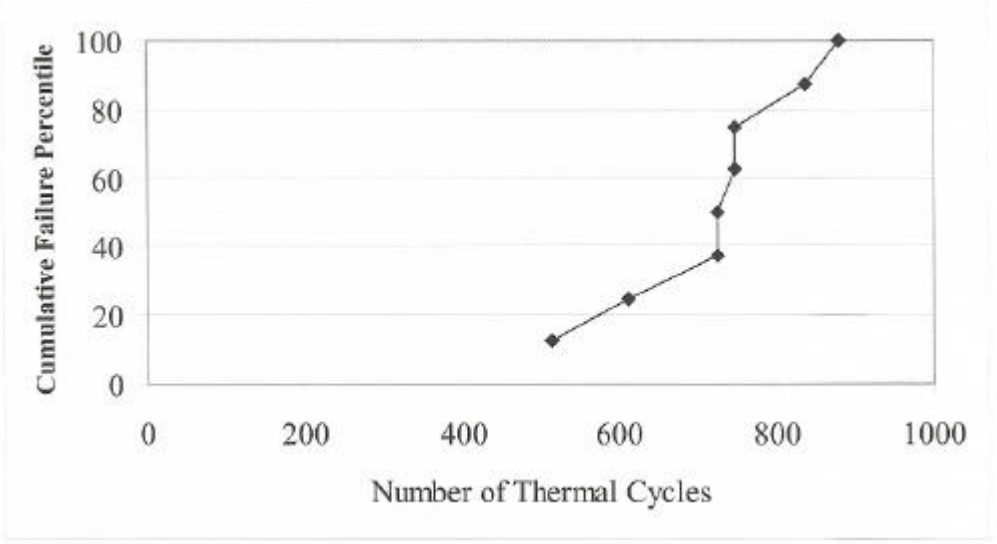

Figure 27. Cumulative cycles-to failure of CB GA on polyimide/glass

The solder joints were severely deformed during the thermal-cycling test. Figure 28 shows corner joints after 100, 270, 500, and 1000 cycles. The two solder joints exposed to 500 and 1000 cycles, respectively, in Figure 28 show that some solder joints were deformed at both the board and the package side, whereas some were basically only deformed at the package side. Furthermore, at the package side, a tongue of solder has pressed itself outwards.

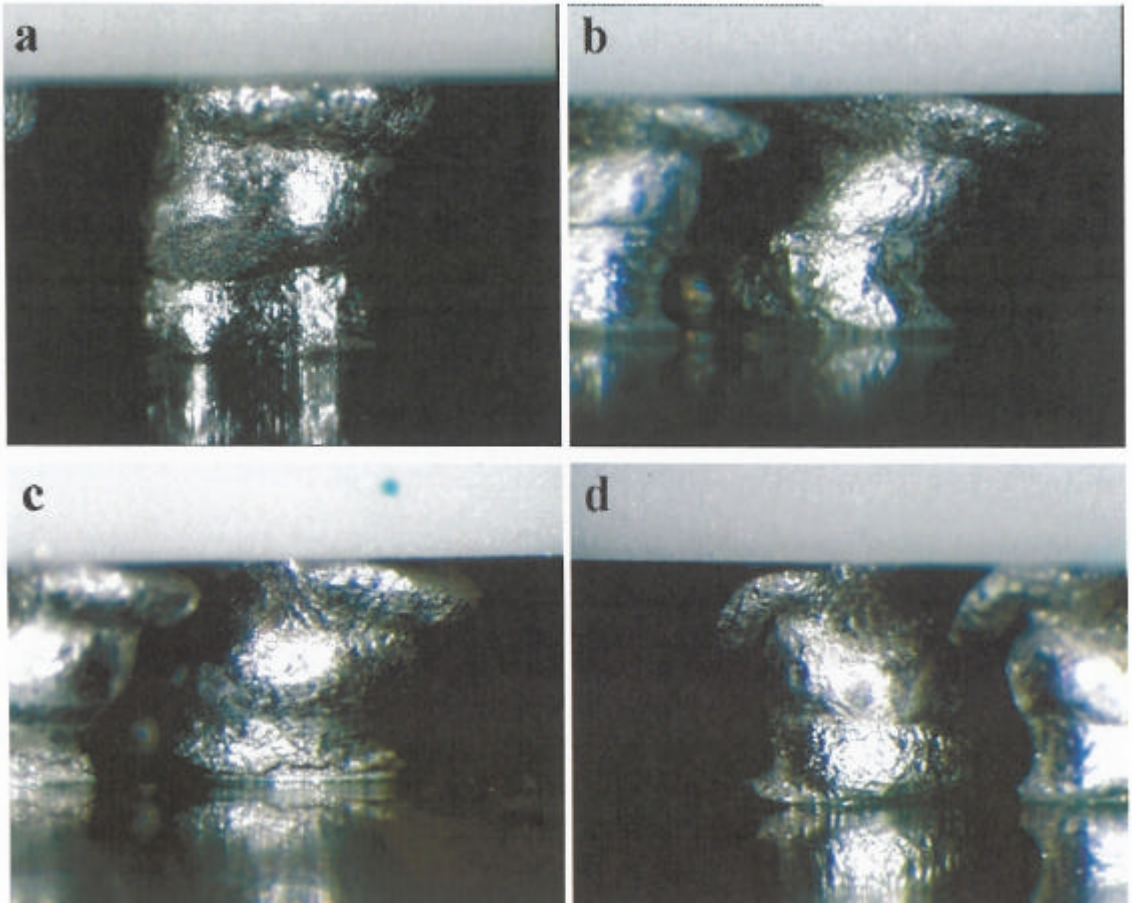

Figure 28. Corner solder joints exposed to 100 cycles (a), 270 cycles (b), 500 cycles (c), and 1000 cycles (d)

Cross-sections of solder joints exposed to 500 cycles are shown in Figure 29. The cut was made diagonally between two corners. Note the big difference in deformation for joints AD 1 and A24 (Figs. 10 and 13 give the coordinates for the ball numbering system). Joint AD1 is deformed both towards the package and the board sides, whereas A24 is basically deformed only towards the package side. Examination of the solder joints that were not deformed towards the board side revealed that cracks had formed in the laminate under the pads (Fig. 30). The cracks are initiated on the inward side of the solder joints. In fact, all solder joints in the outer rows have cracks under the pads, except those pads that are connected to vias located on the inward side of the pads, i.e. the side towards the centre of the package. Thus, a conductor located there prevents the initiation of a crack.

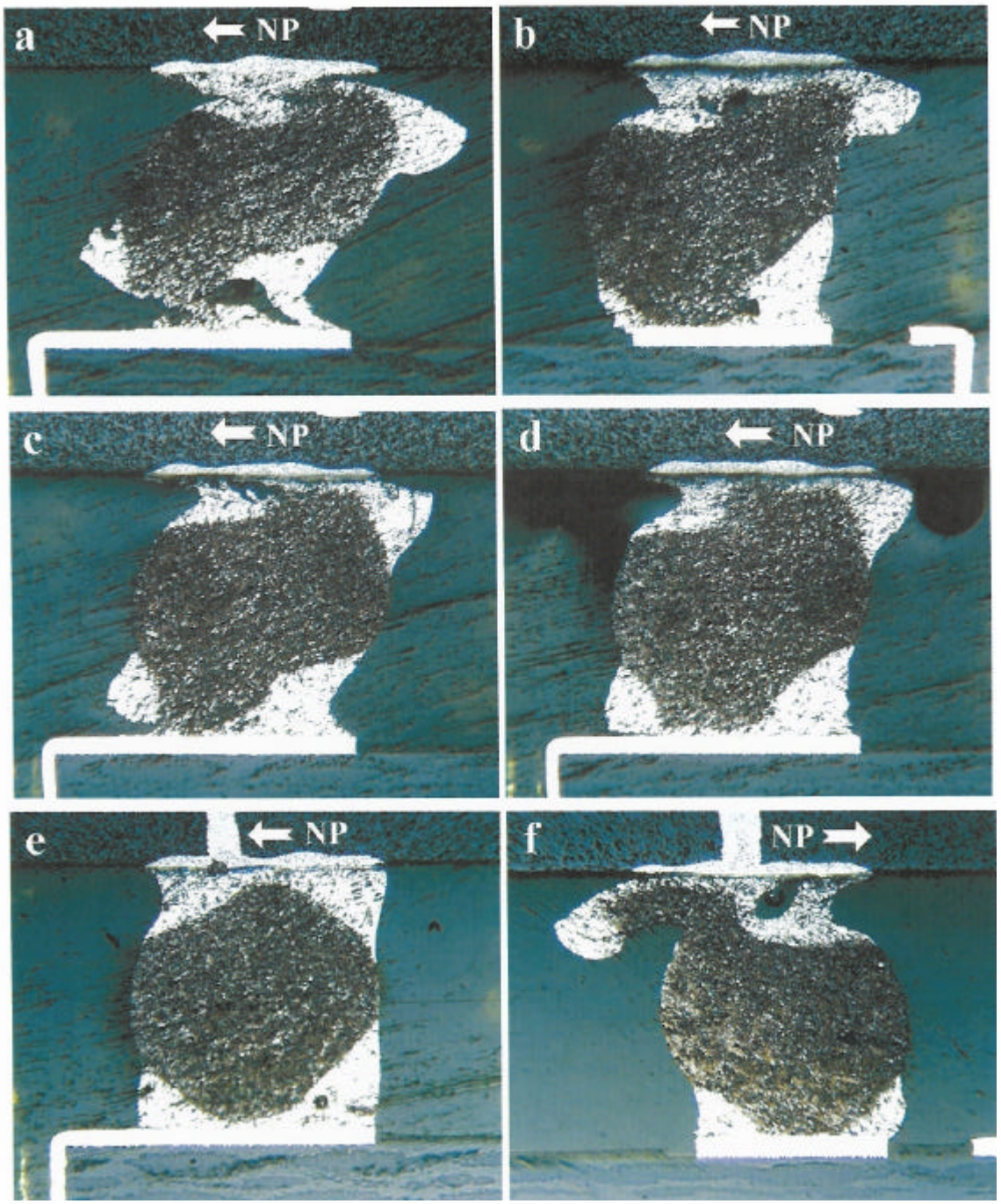

Figure 29. Deformation of solder joints after 500 cycles at positions AD] (a), AC2 (b), AB3 (c), Y5 (d), V7 (e), and A24 (9. The arrows show the direction to the centre of the package, the neutral point (NP)

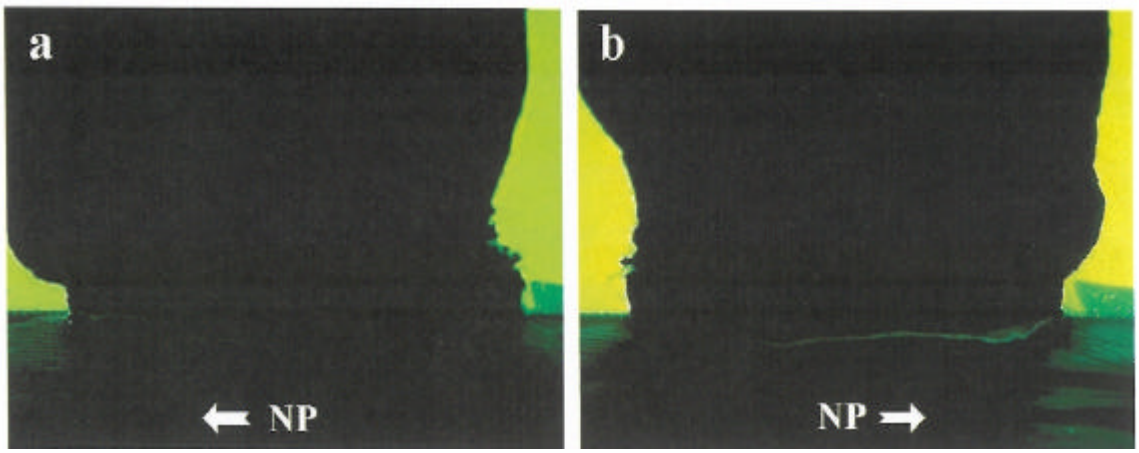

Figure 30. Cracks in the laminate under the pads at positions AC2 (a) and A24 (b)

Analysis of the cracks using dye penetrant after temperature cycling (see Annex A) clearly showed the location and size of the cracks in the solder joints. When removing the packages, the majority of the solder balls remained attached to the board, indicating that the largest cracks in the solder joints were formed between the balls and the pads on the package. Exceptions were the solder joints on the board pads connected inward to vias (Fig. *31).* For these joints, the balls remained on the package.

For some pads on the board not connected to inward vias, the pads were ripped from the laminate. For corner joints, the backsides of the pads were coloured with the dye indicating the presence of a crack in the laminate (Fig. *31).* It was predominantly the inward side of the pads that were coloured, supporting the theory that the cracks initiate on the inward side of the pads.

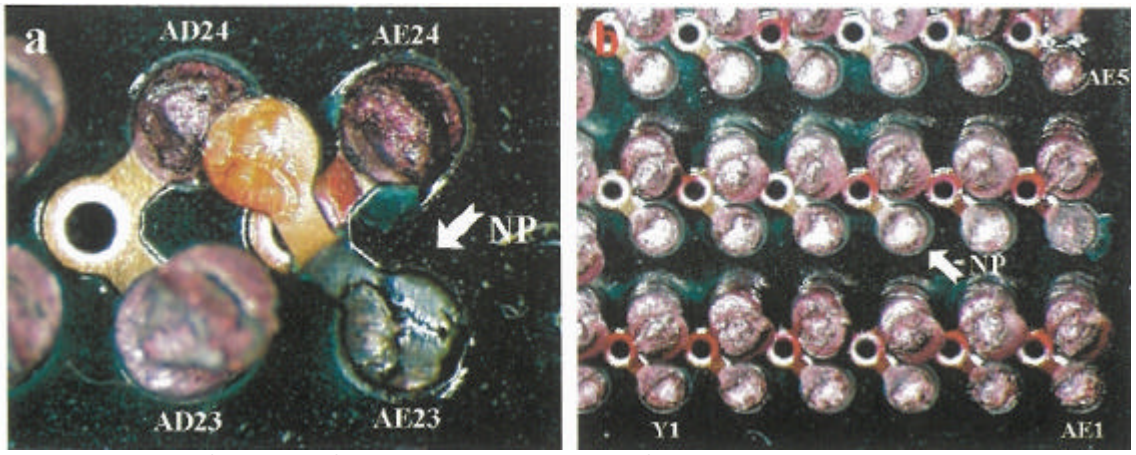

Figure 31. Extent of cracks after 500 cycles (a) and after 1000 cycles (b) analysed using dye penetrant. Ball coordinates are super-imposed on the images

On the package side of a joint, a crack close to the pad/solder interface is formed on the outward side of the joint (Fig. *32).* The "tilting" of the solder ball causes a further reduction in the cross-sectional area from the inward side. This results in the characteristic appearance of partly fractured solder joints as shown in Figure *32.*

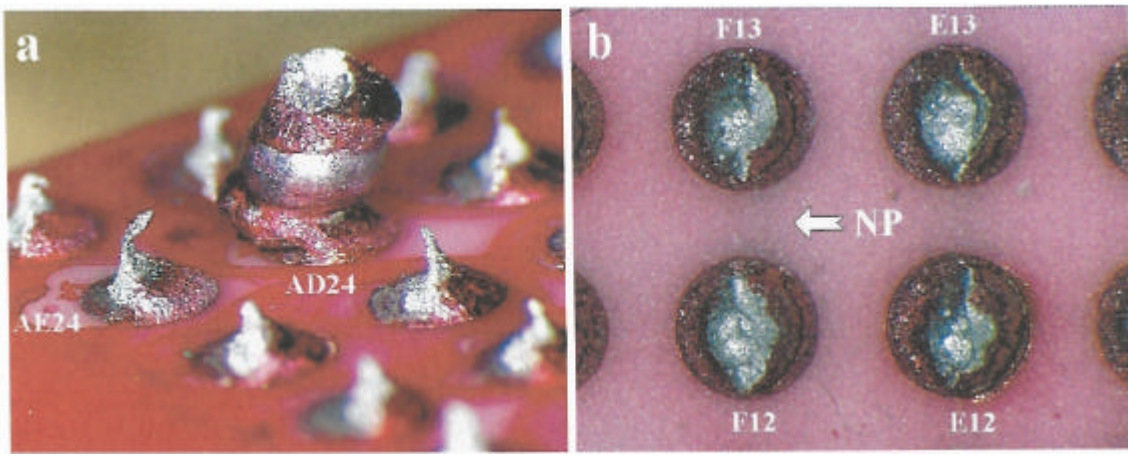

Figure 32. Views showing how the cracks develop on the package side of the solder joints

The formation of cracks on the board side of the solder joint differs from the package side. In this case, the "tilting" of the ball causes a reduction in the solder joint on the outward side of the joint (Fig. 33). This reduction is smaller than on the package side. The crack, which is formed on the inward side, is usually not close to the pad/solder interface.

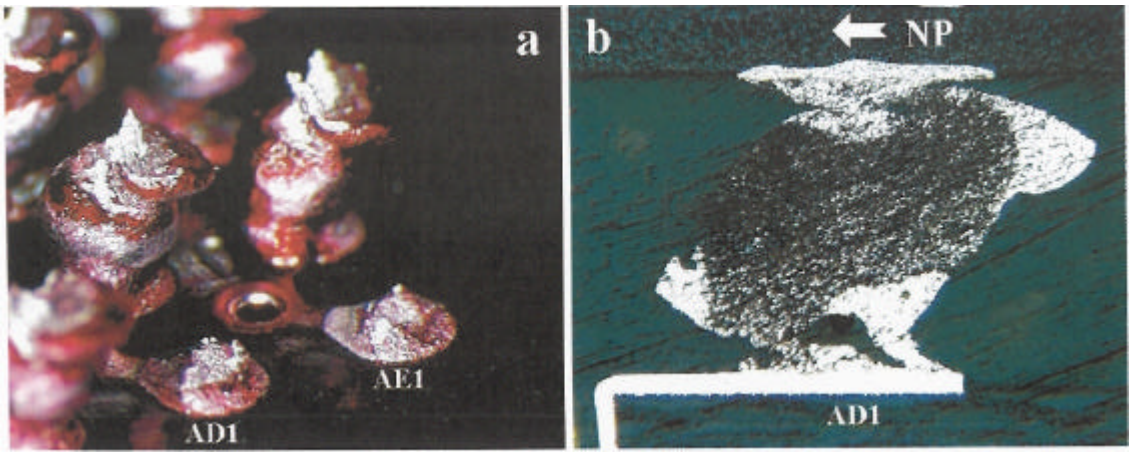

Figure 33. Views showing how the cracks develop on the board side of the solder joints

Closer to the centre of the package, the deformation of the solder joints is very small. Nevertheless, cracks can be found in the solder joints predominantly at the package side close to the pad/solder interface (Fig. 34).

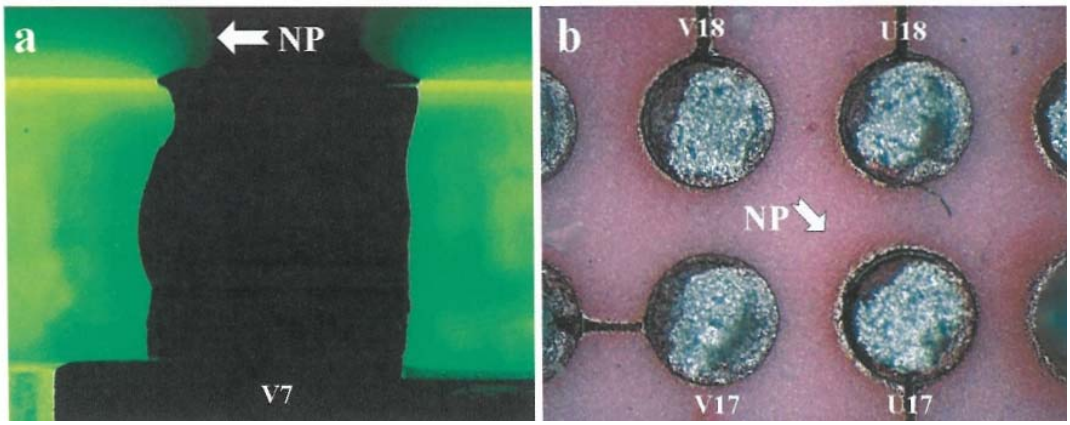

Figure 34. Extent of cracks in solder joints seven and eight rows from the periphery of 'a CBGA after 500 cycles. To the left a cross-section of a solder joint, and to the right cracks developed on the package side of the joints analysed using dye penetrant

Figures 35a and b show the extent of cracking, on the board and package sides, respectively, for corner joints to a CBGA exposed to 500 cycles. Even though some corner joints are completely coloured red, no open circuit event had been registered for this package during the test. Figure 35 also shows the extent of cracking 6 and 9 rows in from the periphery. At row 9 the cracks are very small. Corresponding views of a CBGA exposed to 1000 cycles can be found in Figure 36. After 1000 cycles, the cracks are rather large, even in row 9.

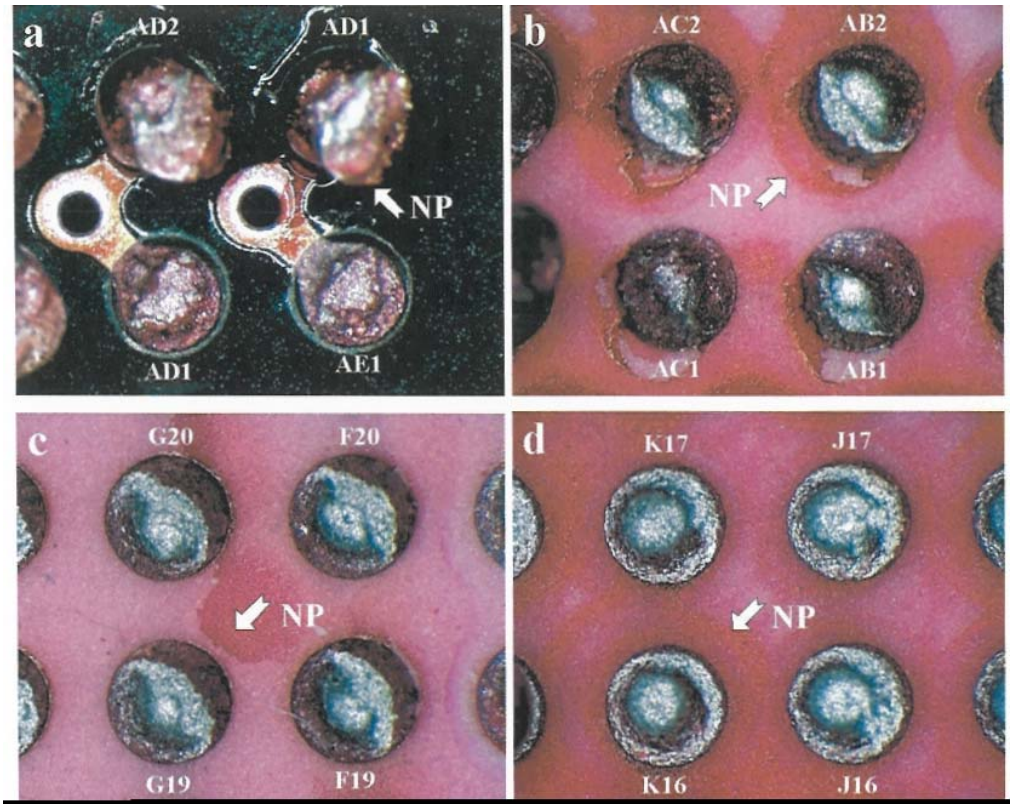

Figure 35. Extent of cracking in solder joints to a CBGA after 500 cycles analysed using dye penetrant on the board side (a) and on the package side (c-d). Ball coordinates are superimposed on the images.

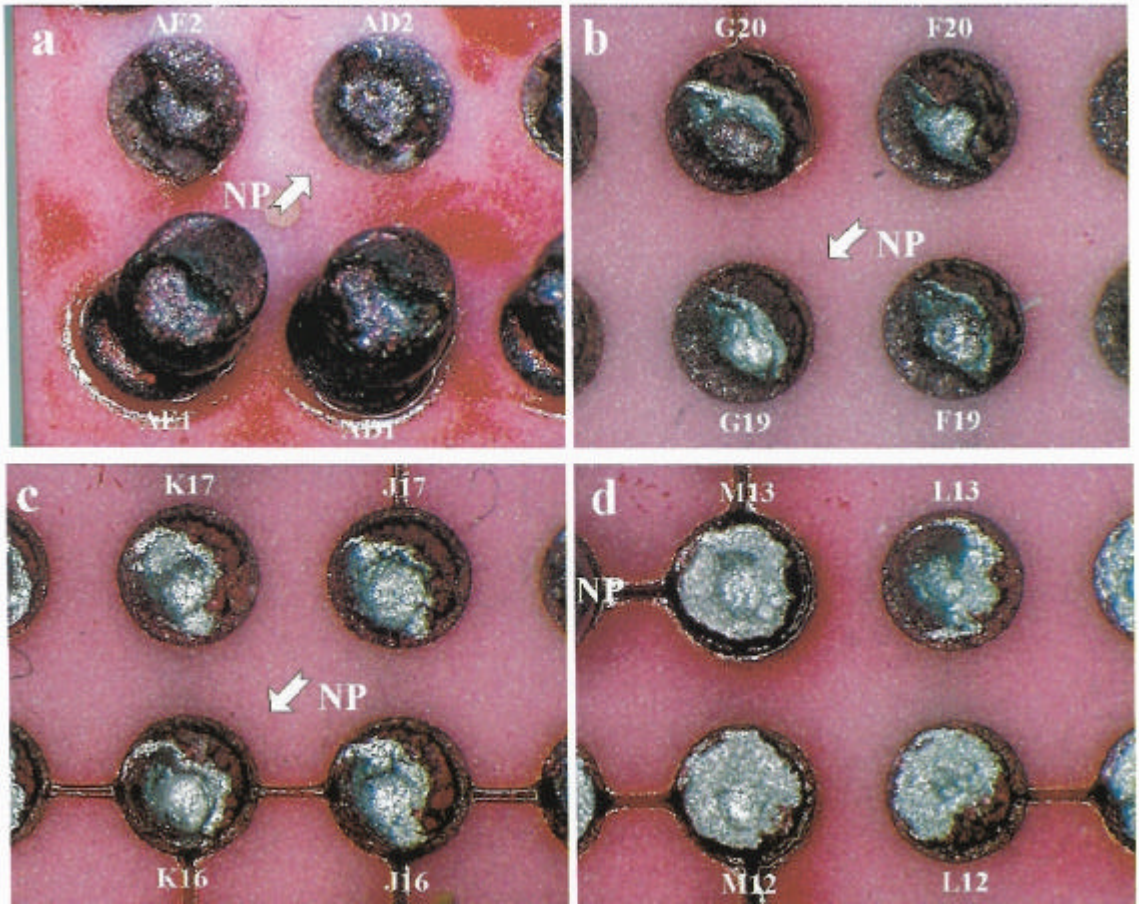

Figure 36. Extent of cracking in solder joints to a CBGA after 1000 cycles, analysed using dye penetrant at various positions on the package side

10.2 Impact of Meagre Solder Joints on Reliability

Four packages with solder paste volume reduced by 44% and eight packages with solder paste volume reduced by 75% for corner joints were cycled to total failure. The results are presented in Figure 37. For the packages with 75% reduced solder paste, only the first failed package of a pair has been registered.

The reduction of the solder paste volume by 75% had a very large impact on the fatigue life of the solder joints, with a reduction in lifetime by a factor of 3 to 5. Even the reduction in the solder paste volume by 44% caused a rather large decrease in the fatigue life, even though the solder fillet diameter was affected very little.

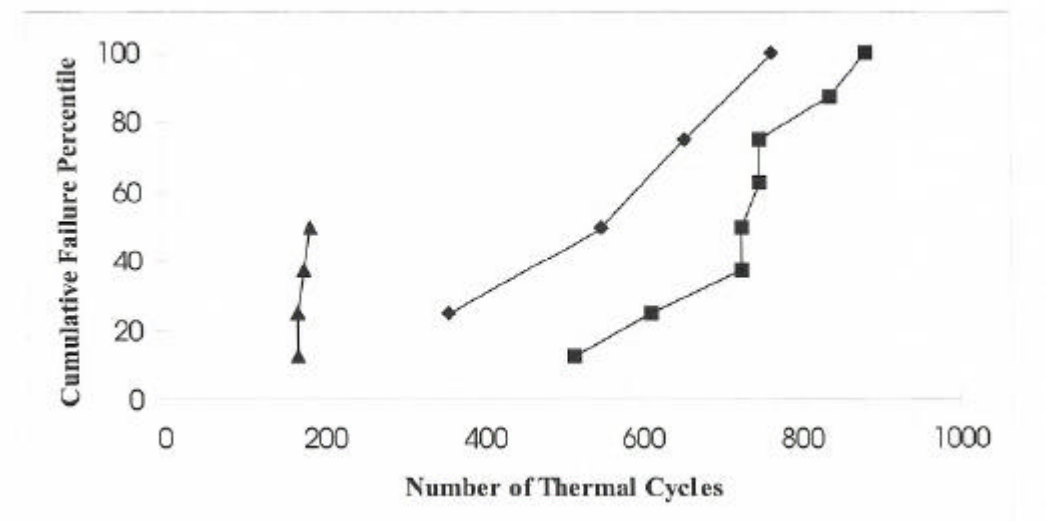

Figure 37. Cumulative cycle-to failure of CBGAs on polyimide/glass boards with 44% (•) and 75% (A) reduced solder paste volume for corner joints, compared to packages with non-reduced solder paste volume (.)

10.3 Reliability Verification Testing

Polyimide/glass Boards

The results from the electrical continuity measurements during the reliability verification testing of the polyimide/glass boards are presented in Table 3 and Figure 38. The cycles-tofailure for all three combinations with CBGAs were of about the same order, and on the same level as in the part evaluating the fatigue mechanism. Thus, neither the additional vibration test during the reliability verification testing nor the application of underfill had any significant impact on the fatigue life of the solder joints.

The only factor that had a significant effect on fatigue life was the exchange of CBGAs for CCGAs. No failures had been registered after 1000 cycles for the CCGAs when no underfill or CV4-2500 was applied. However, rather surprisingly, very early failures were registered for the CCGAs when OHMCOAT 1570 was applied as underfill.

Table 3. Results from the reliability verification testing of CBGAs on polyimide/glass boards

Board No.	Package type	Underfill	Executed cycles	Failed packages	Cycles to failure
P1	CBGA	None	1000	4	452*, 772*
P2	CBGA	None	500	1	478
P3	CBGA	CV4-2500	1000	4	698*, 736*
P4	CBGA	CV4-2500	500	0	-
P5	CBGA	OHMCOAT 1570	1000	3	598*, 610
P6	CBGA	OHMCOAT 1570	500	0	-
P7	CCGA	None	1000	0	-
P8	CCGA	None	500	0	-
P9	CCGA	CV4-2500	1000	0	-
P10	CCGA	CV4-2500	500	0	-
P11	CCGA	OHMCOAT 1570	1000	4	64, 105, 170*

* First failure of a pair of failed packages. The number of cycles to failure for the second package has not been recorded, but was less than 941 cycles

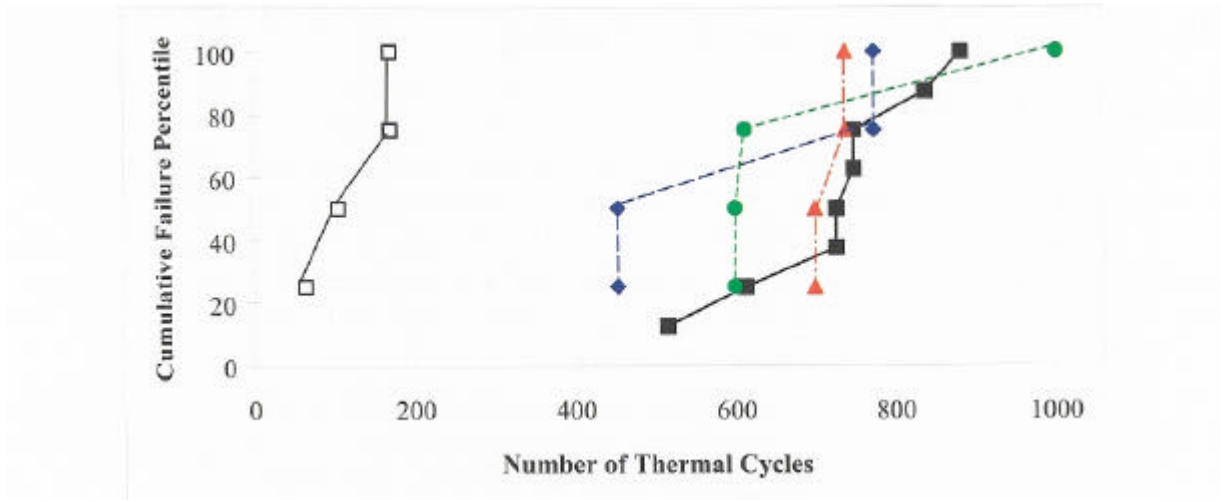

Figure 38. Cumulative cycle-to failure during reliability verification testing of polyimide/glass boards with CBGA/no under fill (.), CBGA/CV4-2500 (4), CBGA/OHMCOAT 1570 O, and CCGA/OHMCOAT 1570 (o). The results from the fatigue mechanism evaluation are shown as a reference (.)

The impact of the reliability verification testing on the integrity of the solder joints was also analysed using cross-sectioning and dye penetrant (only for the package with no underfill). The results from these analyses are reported for each combination of package and underfill type.

CBGA and no Underfill

Cross-sectioning and dye colouring of the boards equipped with CBGAs and no underfill gave the same results as presented in Chapter 10.1. That is, the additional vibration test performed in the reliability verification test had no observable impact on the cracking of the solder joints.

CBGA and CV4-2500 as Underfill

Due to the softness of the CV4-2500 material, it had to be peeled off along the periphery of the packages before they were moulded in epoxy in order to avoid smearing of solder when grinding the samples. However, it was very difficult to completely remove all material and therefore it was difficult to get good cross-sections.

Figure 39 shows a solder joint to a package underfilled with CV4-2500. The deformation and cracking of the solder joint are similar to what was observed for packages without any applied underfill, although the extent of deformation is perhaps slightly less.

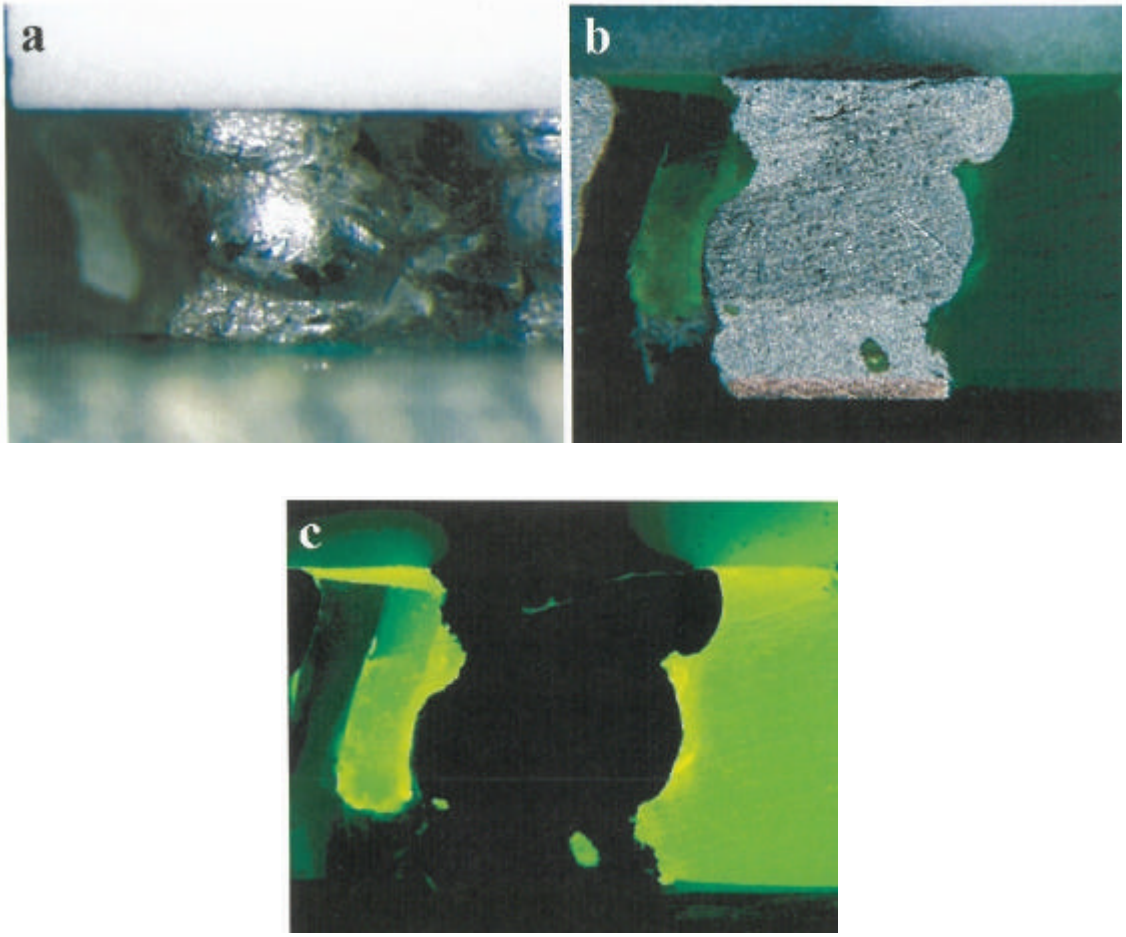

Figure 39. Deformation and cracking of a corner solder joint to a CBGA with CV4-2500 as underfill on polyimide/glass after 1000 cycles. Views (b) and (c) show cross-sections of the solder joint taken with ordinary light and "black light", respectively

CB GA and OHMCOA T 1570 as Underfill

No deformation of the solder joints was observed for the packages underfilled with OHMCOAT 1570 (Fig. 40). However, after 500 cycles, delamination between the underfill material and the package, and cracks close to the package pad, were observed (Fig. 41). After 1000 cycles, the gap between the underfill material and the package had expanded and corner joints were completely cracked. No delamination was observed between the underfill material and the board. At some solder joints, a crack going downward in the board material was observed. These cracks were initiated at the edge of the solder lands (Fig. 42).

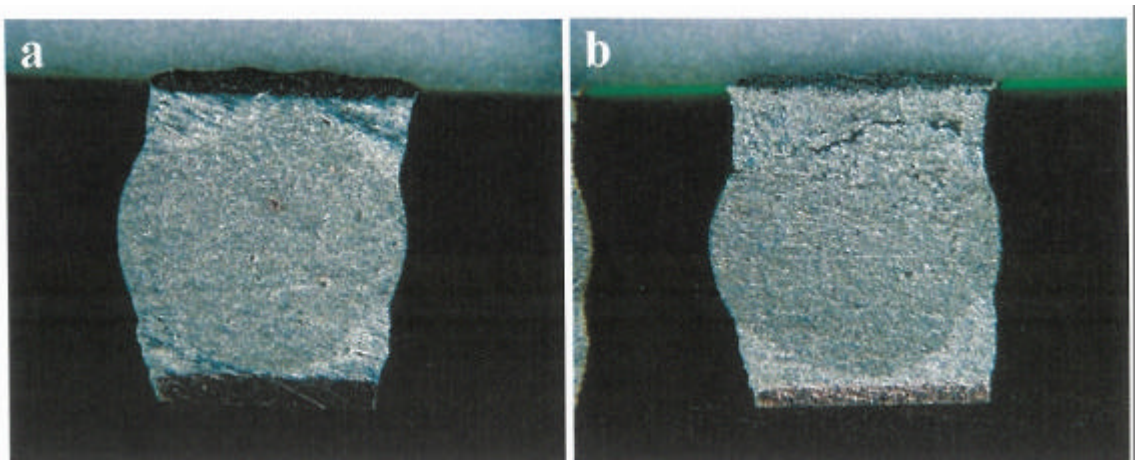

Figure 40. Cross-sections of corner solder joints to CBGAs underfilled with OHMCOA T 1570 on polyimide/glass after 500 cycles (a) and after 1000 cycles (b)

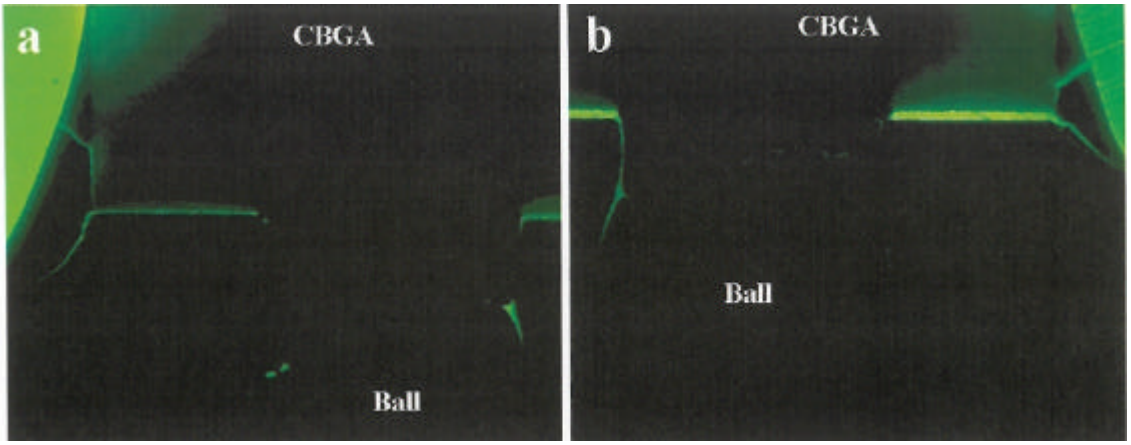

Figure 41. Cross-sections of corner solder joints to CBGAs underfilled with OHMCOAT 1570 on polyimide/glass showing delamination between the underfill material and the package, and cracks close to the package pad formed after 500 cycles (a) and after 1000 cycles (b)

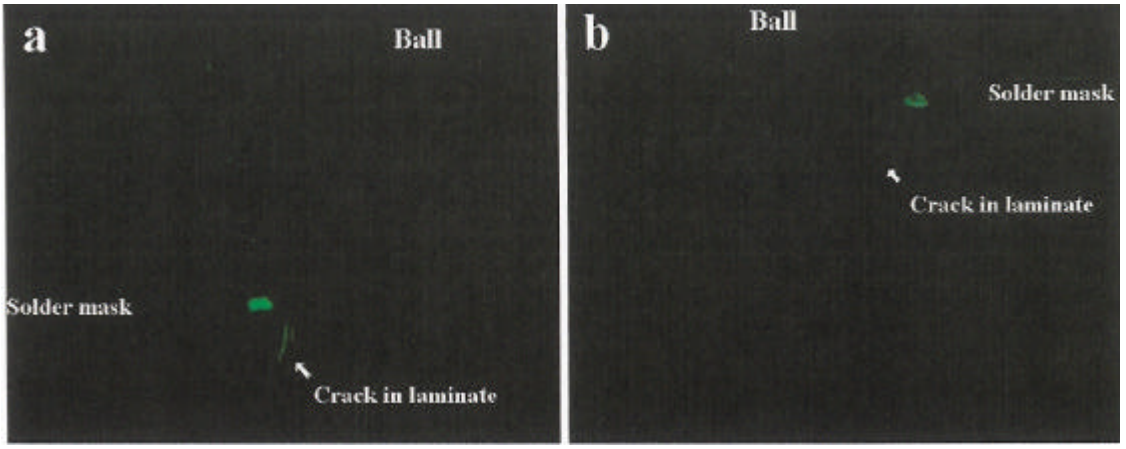

Figure 42. Cross-sections of solder joints to CBGAs underfilled with OHMCOAT 1570 on polyimide/glass showing cracks in the board laminate formed after 500 cycles (a) and after 1000 cycles (b)

CCGA and no Underfill

The columns on the CCGAs showed the typical deformations after the thermal cycling reported by IBM [39]. The deformations were located towards the top of the eutectic fillets at the joints to both the package and the board lands (Fig. 43). Cracks are also formed in the deformed locations (Fig. 44). Figure 45 shows the extent of cracks in fractured joints analysed with dye penetrant. No cracks were found in the laminate beneath the pads on the board.

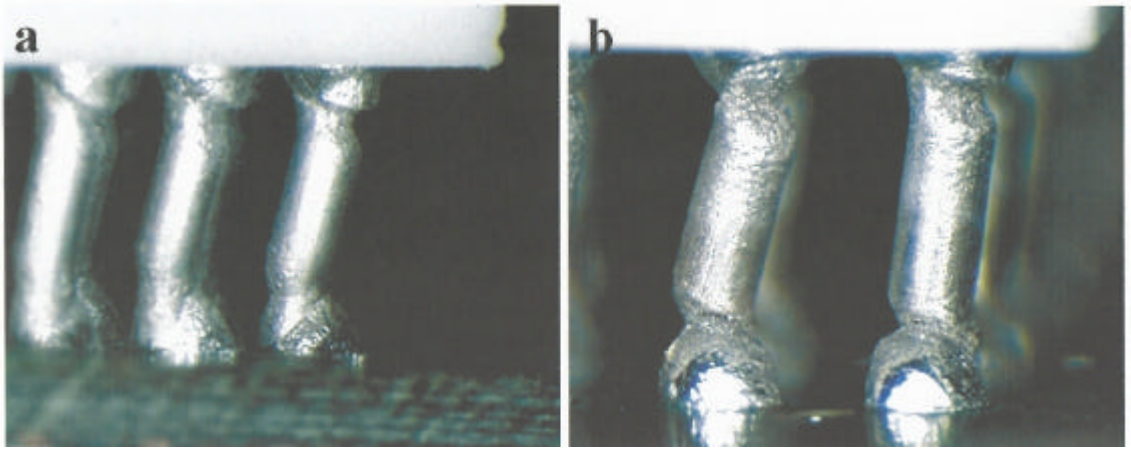

Figure 43. Deformation of corner columns to CCGAs on polyimide/glass after 500 cycles (a) and after 1000 cycles (b)

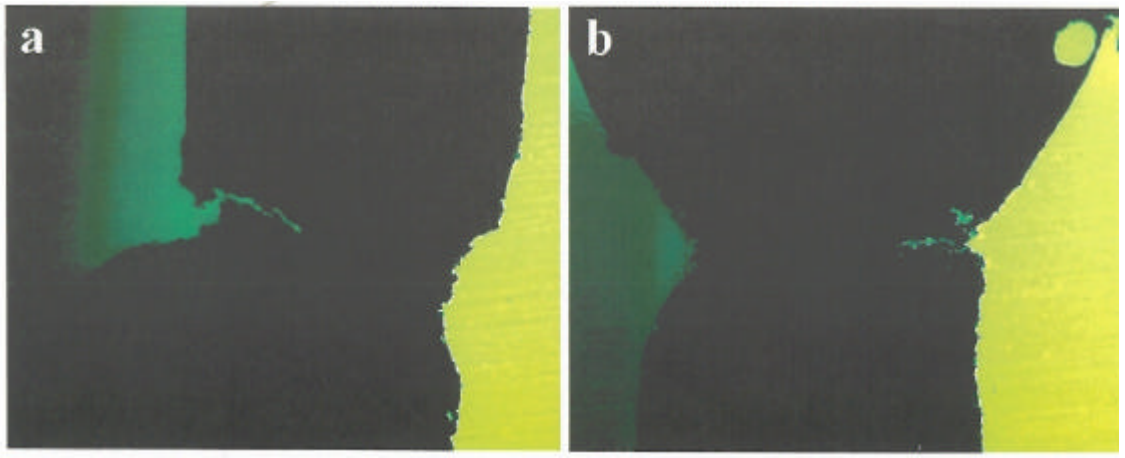

Figure 44. Cracks in the corner column shown in Figure 43b on the board side (a) and on the package side (b)

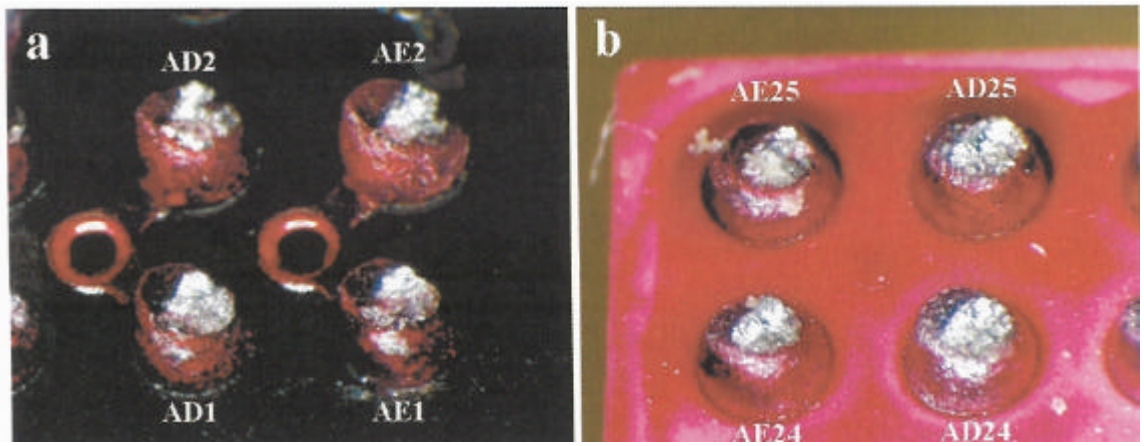

Figure 45. Extent of cracking in corner columns after 1000 cycles on the board side (a) and on the package side (b) analysed using dye penetrant

CCGA and CV4-2500 as Underfill

The results for the CCGA packages underfilled with *CV4-2500* were practically identical to the results for the packages without any underfill (Fig. *46)*.

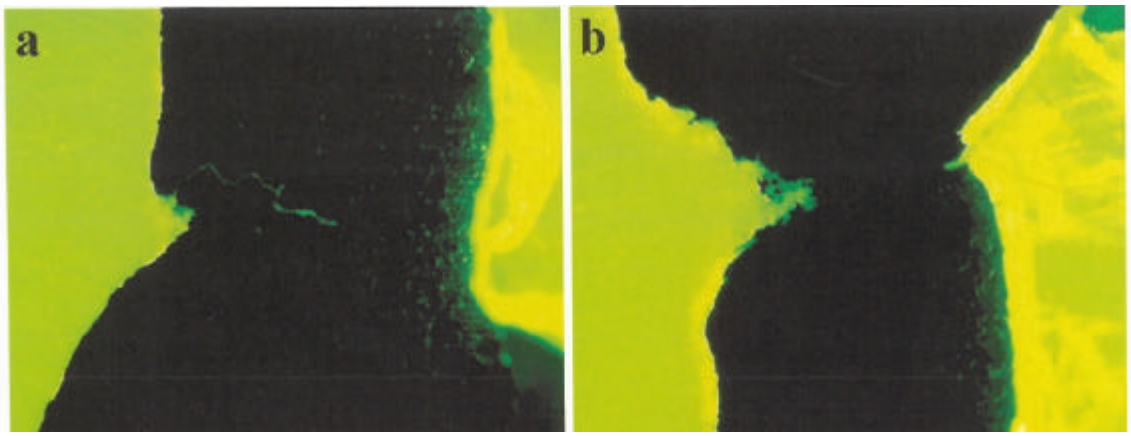

Figure 46. Deformation and cracks in a corner column to a CCGA underfilled with CV4 2500 on the board side (a) and on the package side (b) after 1000 cycles

CCGA and OHMCOAT 1570 as Underfill

Use of OHMCOAT *1570* as underfill caused severe delamination between the underfill and the package, resulting in very early fracturing of the solder joints (Fig. *47).* The cracks occurred in the fillets towards the package pads, and the early failures indicate a very fast cracking process.

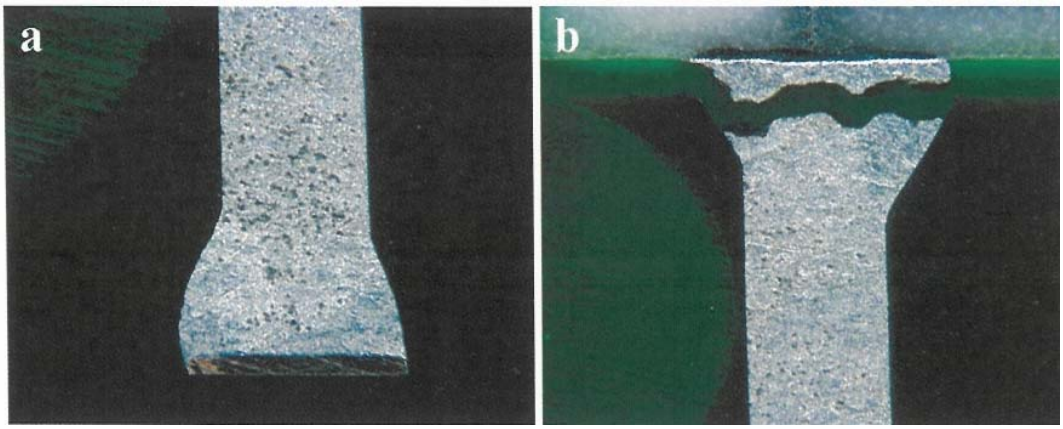

Figure 47. Cross-section of corner column of a CCGA under f lled with OHMCOAT 1570 showing the board (a) and the package (b) sides of the joint

Thermount Boards

The reliability of CBGAs and CCGAs was improved considerably by the use of Thermount boards instead of polyimide/glass boards. Only for the CCGA and OHMCOAT *1572* combination were failures recorded during the temperature-cycle testing of the Thennount boards. For this combination, six of the seven packages failed during cycles 97 or 98 and the remaining during the vibration test performed after 100 cycles. The integrity of the solder joints analysed using cross-sectioning and dye penetrant are reported for each combination of package and underfill type.

CBGA and no Underfrll

In contrast to CBGAs mounted on Polyimide/glass, practically no deformation at all was observed in the solder joints for the CBGAs mounted on Thermount (Fig. 48). Nevertheless, cracks had formed close to the package pads (Figs. 49 and *50).* No cracks could be seen on the board side of the solder joints, but extensive cracking was observed in the laminate beneath the corner lands (Fig. *51).*

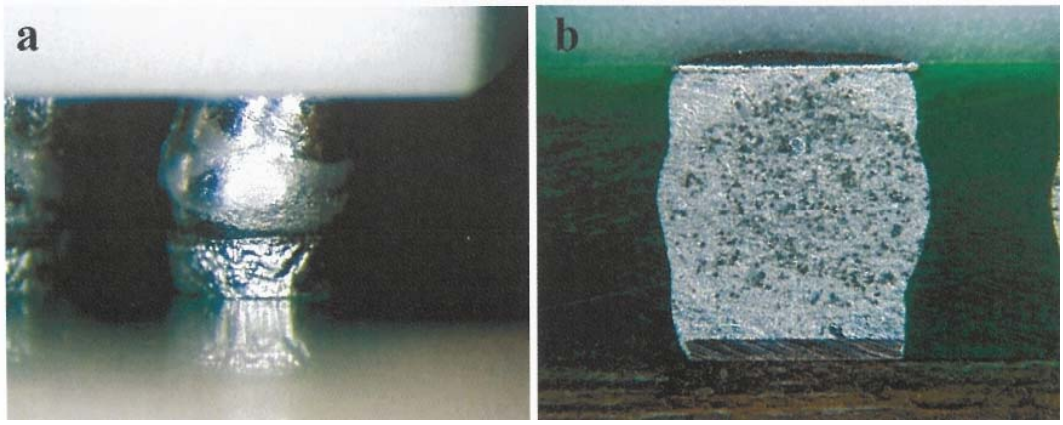

Figure 48. Views of corner solder joints to a CBGA mounted on Thermount after 1000 cycles

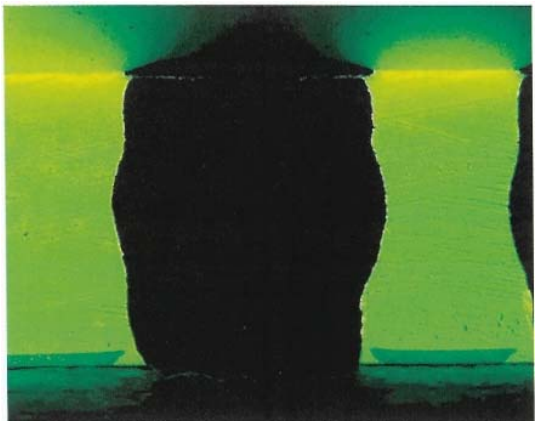

Figure 49. Cross-section of a corner solder joint to a CBGA mounted on Thermount after 1000 cycles

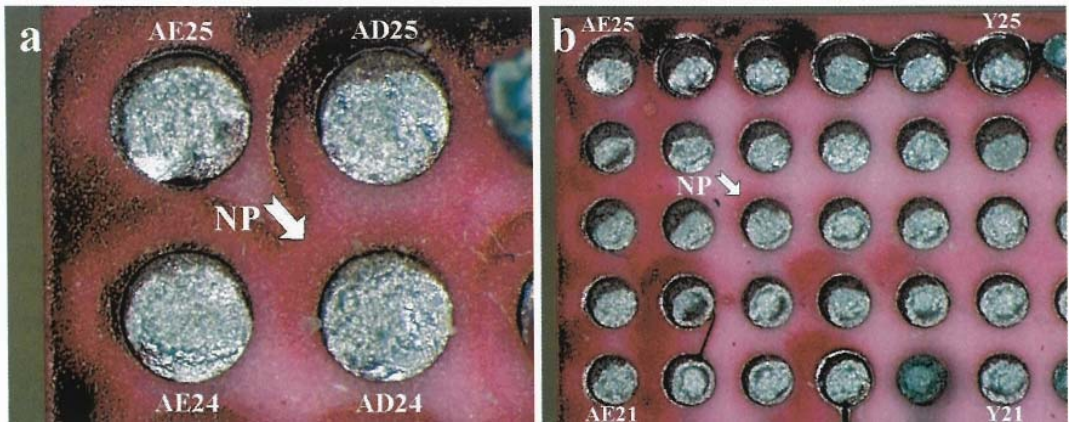

Figure 50. Extent of cracking in corner solder joints to CBGAs mounted on Thermount after 500 cycles (a) and after 1000 cycles (b)

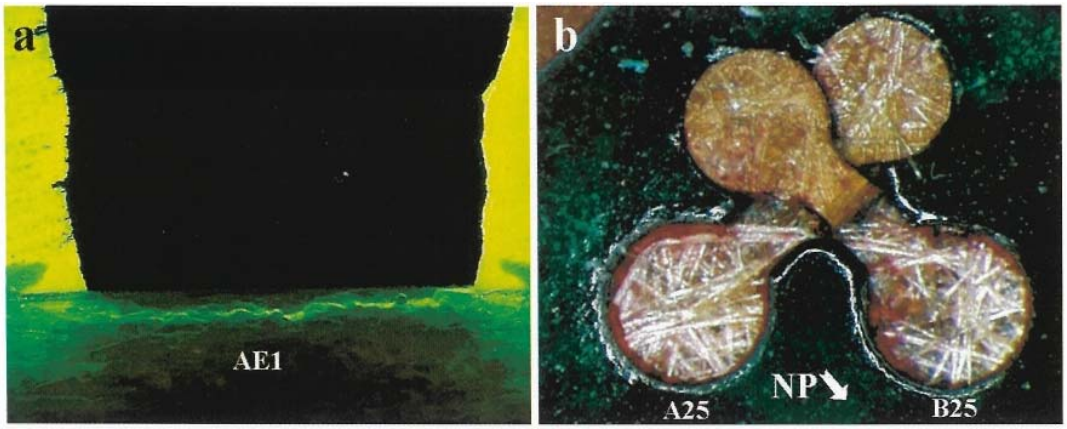

Figure 51. Cracking in the Thermount laminate beneath solder pads to corner joints after 1000 cycles. View (b) shows pads ripped off after colouring with the dye penetrant

CBGA and CV4-2500 as Underfill

Due to the difficulties in examining the packages underfilled with *CV4-2500* using cross-sectioning and dye penetrant, these packages have not been analysed. However, since *CV4-2500* had a negligible effect when applied as underfill on the polyimide/glass boards, the same can be expected on the Thermount boards.

CBGA and OHMCOAT 1572 as Underfll

Delamination between the OHMCOAT material and the package was observed also for the Thermount boards (Fig. 52). Cracks were found both on the package and on the board sides of the joints (Fig. 53). The cracks were formed in the ball region. Furthermore, delamination had occurred between the underfill material and the solder mask between some solder joints, predominantly between solder joints connected to the same via. Between other solder joints, cracking had instead occurred in the laminate beneath the solder mask (Fig. 54). No cracks were observed beneath the solder lands.

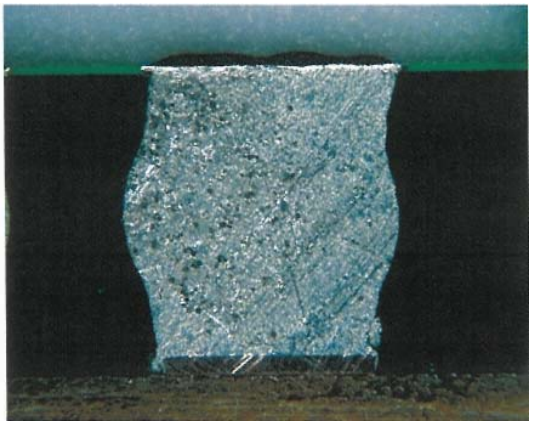

Figure 52. Cross-section of a corner solder joints to a CBGA mounted on a Thermount board and underfilled with OHMCOAT 1572 after 1000 cycles

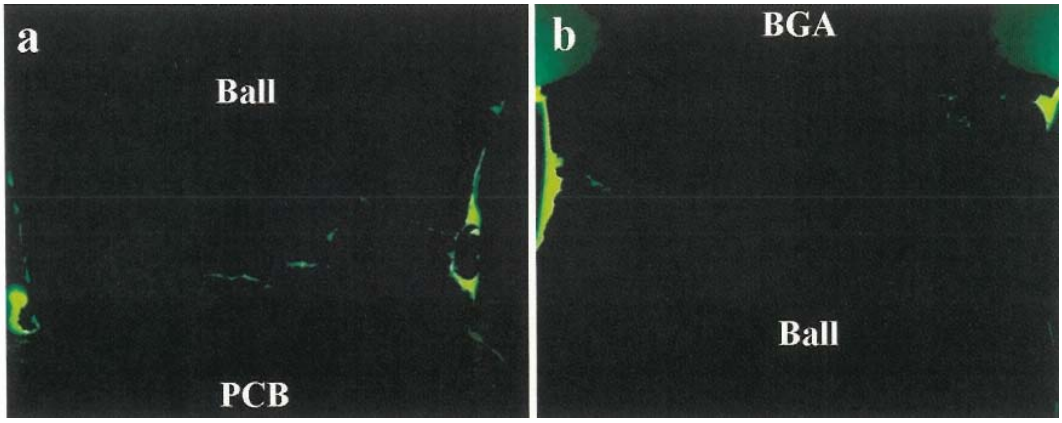

Figure 53. Cracking after 1000 cycles in solder joints to a CBGA mounted on a Thermount board and underfilled with OHMCOAT 1572 on the board (a) and the package sides (b) of the joints, respectively

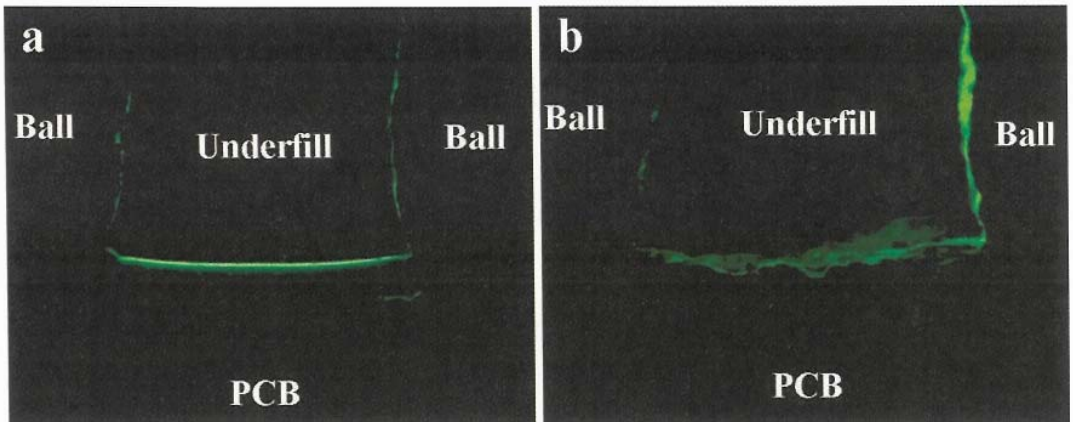

Figure 54. Delamination after 500 cycles between underfall and solder mask (a) and cracking in laminate (b) between solder joints to a CBGA mounted on a Thermount board and underfilled with OHMCOA T 1572

CCGA and no Underfrll

The columns on the CCGAs were seemingly unaffected after the thermal cycling (Fig. *55)* and no cracks were found in the solder joints (Fig. *56)*.

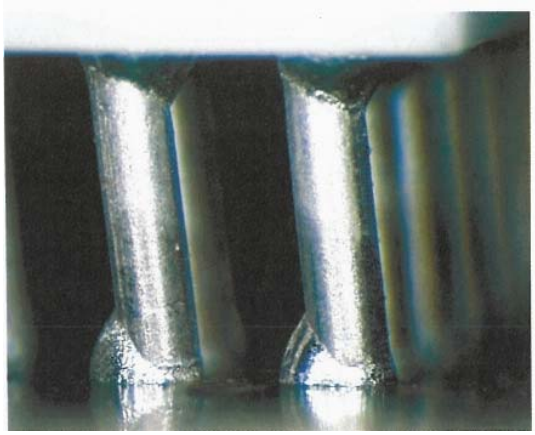

Figure 55. View of corner columns on a CCGA mounted on a Thermount board that had been exposed to 1000 cycles

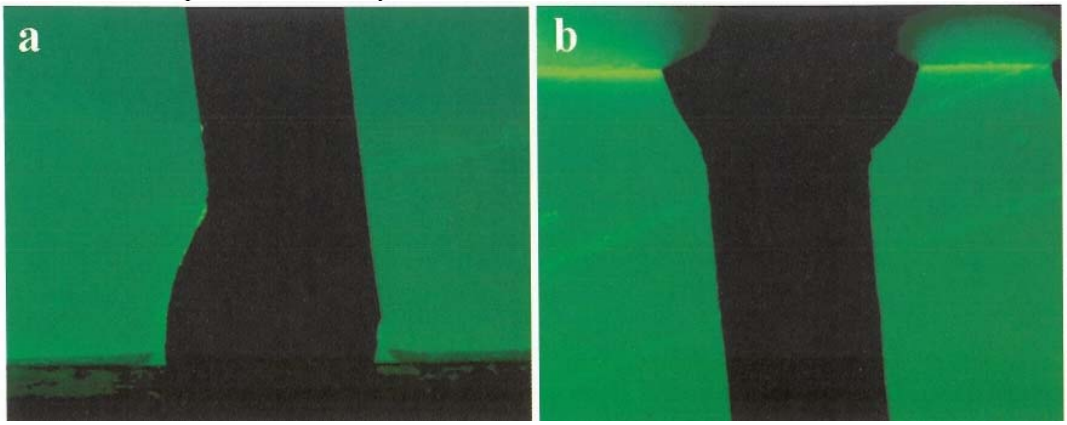

Figure 56. Cross-sections of 'a corner column to a CCGA mounted on a Thermount board after 1000 cycles showing the solder joints towards the board side (a) and the package side (b)

CCGA and CV4-2500 as Underfill

The results for the CCGAs underfilled with CV4-2500 have not been investigated, but are expected to be similar to the results for the packages without any underfill.

CCGA and OHMCOA T 1572 as Underfill

As for the polyimide/glass boards, use of OHMCOAT as underfill caused severe delamination between the underfill and the package, resulting in fracturing of the solder joints (Fig. 57). Delamination also occurred between the underfill material and the board, although no cracking of the solder joints was found in the fillets to the board.

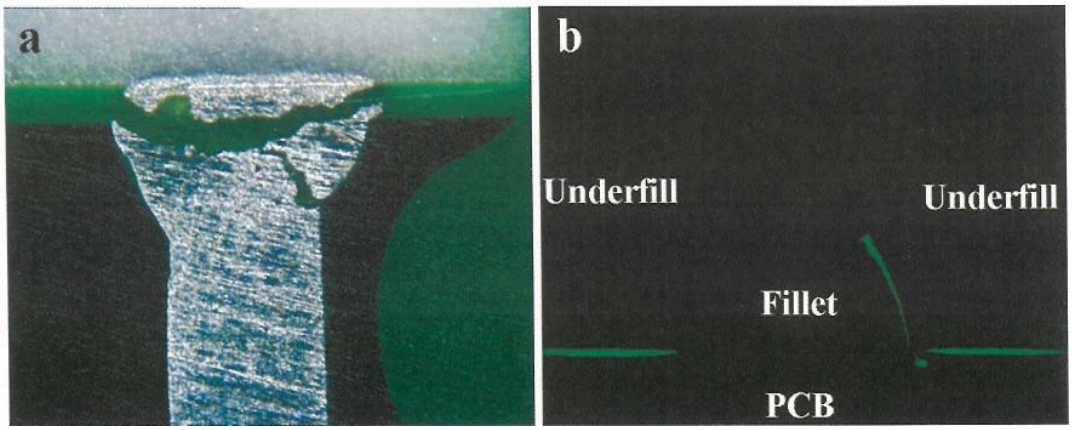

Figure 57. Cross-sections of columns to a CCGA mounted on a Thermount board, underfilled with OHMCOAT 1572 and exposed to 500 cycles. These views show the solder joint to the package side for one of the columns (a) and the solder joint to the board side for the other column (b)

11 Conclusions

1 According to the European Space Agency's requirements specification for surface mount technology (SMT), ESA PSS-01-738 [43], a configuration is considered verified if there are no cracked joints or package damage after exposure to 500 thermal cycles and vibration testing per ECSS-Q-70-08A, Chapter 13 [48]. Surface cracks that penetrate less than 5% of the solder fillet or less than 20 micrometers in depth are considered acceptable. Ceramic BGAs with 625 I/Os soldered to polyimide/glass are very far from passing this requirement. In fact, some packages failed before 500 cycles and those that had not failed after 500 cycles had solder joints that were almost completely cracked through. Since the distance of a solder joint to the centre of the package is crucial for the fatigue life, packages with smaller size would have longer fatigue life. The extent of cracking at various locations indicates that a CBGA package needs to have less than 200 I/Os (with unchanged pitch) to pass the acceptance requirement.

2 Application of the silicone material, CV4-2500, had no significant impact on the reliability of the solder joints, neither negative nor positive. Probably, it is too soft to affect the distribution of mechanical stresses due to mismatch of the CTEs for the various materials. This is supported by the results of a previous ESA study which confirmed that thick silicone conformal coatings had little effect on the thermal fatigue life of either SMT or through hole soldered joints. Polyurethane and epoxy conformal coatings had a progressively negative effect [50].

The epoxy underfill prevented the deformation of the solder joints to CBGAs soldered to polyimide/glass but had no measurable effect on the fatigue life of the solder joints. However, it cannot be excluded that an underfill with other properties (CTE, modules, etc.) might have improved the fatigue life. The adhesion of the underfill to board, solder, and ceramic might also be important [51]. Cross-sections of solder joints after testing showed that the underfill had delaminated from the ceramic substrate in the CBGAs.

3 Substitution of the balls on the packages for columns improved the fatigue life considerably of packages soldered to polyimide/glass. No failures had been registered after 1000 cycles. Thus, the improvement in fatigue life is at least doubled. Nevertheless, the deformation of the solder columns is considerable after 500 cycles and CBGAs mounted on polyimide/glass do not pass the acceptance requirement in ESA PSS-01-738. However, a smaller package would probably pass.

4 As for the CBGA, application of CV4-2500 beneath CCGA soldered to polyimide/glass had no significant impact on the reliability of the solder joints. By contrast, the epoxy underfill caused a catastrophic decrease of the fatigue life. This should perhaps have been expected. The purpose of replacing the balls with columns is to give more flexibility to the interconnections between package and board. By applying an underfill, this flexibility is ruined.

5 The low CTE values in-plane for Thermount 85NT improved the fatigue life considerably for both CBGAs and CCGAs. Most remarkably, no defonnation occurred for the solder joints to the CBGAs. Nevertheless, cracks formed in the solder joints, predominantly towards the package pads. The reason why the cracks formed predominantly at the package pads is probably that the stresses there are due to a combination of global mismatch (package/board) and a local mismatch (solder/ceramic) of CTEs. The local mismatch at board pads between solder and board laminate is much less. Thermount 85NT has recently been approved as a laminate suitable for space-use according to the requirements of ESA [44].

6 For the CBGAs, the cracks that formed in corner joints penetrated up to 20% of the solder fillet after 500 cycles and up to 50% after 1000 cycles. Thus, CBGAs mounted on Thermount 85NT were on the borderline to pass the acceptance requirement in ESA PSS-01-738. Although the cracks are larger than acceptable, it is a considerable improvement when comparing with polyimide/glass boards. The improvement in fatigue life is probably in the order of at least a factor of four.

7 The only combination of package and board substrate that passed the acceptance requirement in ESA PSS-01-738 was CCGAs mounted on Thermount 85NT. No deformation or cracks were detected in the solder interconnections even after 1000 cycles for this combination.

8 The application of an epoxy underfill beneath both CBGAs and CCGAs mounted on Thermount 85NT caused faster cracking, especially for the CCGAs. Again, this was probably due to the fact that an underfill impairs the flexibility of the solder interconnections.

9 The amount of solder paste printed on the solder pads is very critical for the fatigue life of the solder joints to CBGAs. A decrease of the solder paste volume to 0.068 mm^3, about 10% less than the minimum solder paste volume recommended by IBM, caused a decrease of the fatigue life with 20-40%. This decrease occurred even though the appearance of the solder fillet was not much affected. The change in solder fillet geometry is probably too small to be detected with any X-ray technique. Therefore, it will be

difficult to verify adequate solder fillet geometry using any inspection method. A teardrop design of the pads maybe could be used to indicate a "surplus" of solder. Anyhow, paste volume measurements are strongly recommended to minimise the risk for insufficient solder paste volumes resulting in meagre solder joints. Too little solder paste printed on a single pad due to, for example, clogging of the stencil, could dramatically reduce the reliability of the package. Since warpage will also cause reduced solder fillet diameter, measures should be taken to ascertain that warpage will be at an acceptable level.

10 Laminate cracking occurred beneath board pads to CBGAs mounted on both polyimide/glass and Thermount 85NT. Such failure is thought to be caused by thermal mechanical stress during reflow and/or subsequent mechanical stresses on the joints [Section 8.4 in Ref. 2]. Since cracks were not present beneath the solder pads to the packages underfilled with epoxy, the cracks must have formed during the thermal cycling. It should be noted that cracks formed in the laminate also when the packages were underfilled with epoxy, but then between the solder pads. Clearly, the epoxy underfill caused a redistribution of the stresses although this did not improve the fatigue life of the solder joints.

Cracks were also found in the laminate on boards that were used for the initial assessment of the soldering process (Fig. 58a). Since the boards used for assessing the soldering process had not been thermally cycled, there must be another cause for the cracks on these boards. Bending of the boards during handling may have caused the cracking. Although the boards had not been handled especially carelessly, they had been handled to a larger extent than the boards used in the main study. Another difference was that the boards used for assessment of the soldering process had not been baked prior to soldering. Thus, a plausible explanation for the cracking is that a higher water content in the laminate causes a "pop-corn" type of failure mechanism. This latter explanation is supported by the finding that one pad seems to have "popped up" during soldering (Fig. 58b). Whatever the reason why the cracks formed, these findings demonstrate the higher vulnerability for this type of failure when using BGA packages compared to components with leads. This early failure mode must also be considered when evaluating the reliability of BGA packages.

Since cracks in the laminate beneath pads will decrease the mechanical stress on the solder joints during thermal cycling, they actually improve the fatigue life of the solder joints. However, they may increase the risk for other failure mechanisms. If the connection to the pads is achieved by via-in-pads, the copper barrel in the via holes may crack causing open circuits (see Annex B). Ingress of humidity and ionic contamination in the cracks may also cause short circuits due to formation of conductive anodic filaments [52, 53].

11 The suitability of a "destructive dye penetrant" test method for quantifying the extent of thermal fatigue cracks within soldered interconnects was demonstrated. This procedure has been documented. It is likely to supplement all the X-ray system inspection and metallographic methods that were recently evaluated by ESA for BGA assemblies [41].

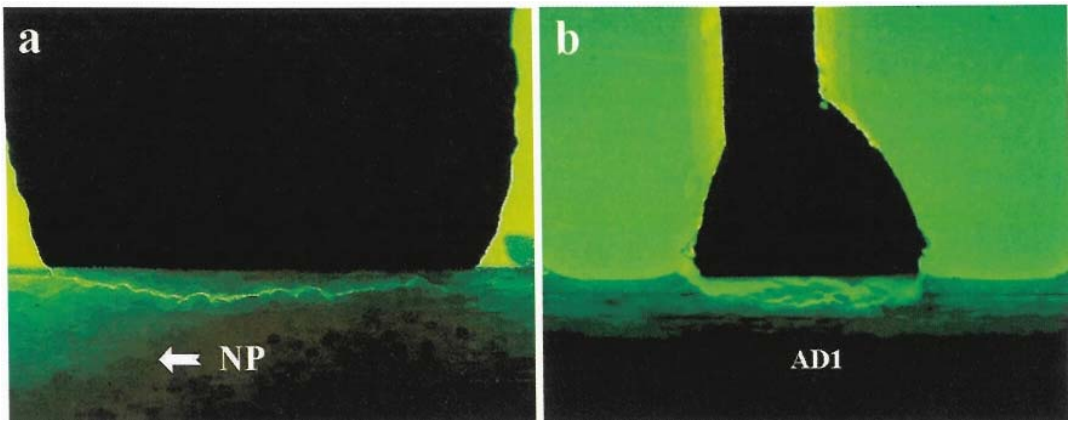

Figure 58. Views showing defects on a board used for verifying the soldering process. View (a) shows a crack in the Thermount 85NT laminate under a corner solder joint and view (b) shows a pad that has 'popped up"

12 Acknowledgements

The work performed in this report was funded by the European Space Agency through its European Space Research and Technology Centre. The authors would also like to acknowledge Mr. Bernard Jouineau of Astrium Space, Velizy, France for preparing some of the test BGA assemblies, and thank Dr. Reza Ghaffarian of the NASA Jet Propulsion Laboratory, Pasadena, USA for reviewing our text.

13 References

1 M. S. Cole and T. Caulfield, *Ball Grid Array Packaging,* Proc. Surface Mount International, 1994, pp. 147-153.

2 IPC-7095, *Design and Assembly Process Implementation for BGAs, IPC,* Aug 2000.

3 M. S. Cole and T. Caulfield, *A review of Available Ball Grid Array (BGA) Packages,* Proc. Surface Mount International, 1995, pp. 207-213.

4 R. Ghaffarian, *Ball Grid Array Packaging Guidelines,* Jet Propulsion Laboratory, California Institute of Technology, Distributed by Interconnection Technology Research Institute (ITRI), August 1998.

5 P. M. Hall, Solder Post Attachment of Ceramic Chip Carriers to Ceramic Film Integrated Circuits, *IEEE Trans. Components, Hybrids, and Manufacturing Technology, Vol.* 4, No. 4, 1981, pp. 403-410.

6 D. R. Banks and R. D. Gerke, *Assembly and Reliability of Ceramic Column Grid Array,* Proc. Surface Mount International, 1994, pp. 271-276.

7 J-STD-013, *Implementation of Ball Grid Array and other High Density Technology,* IPC, July 1996.

8 R. Lanzone, *Dimple Ball Grid Array (D-BGA): A New CBGA Package,* Proc. Nepcon West, 1996, pp. 657-677.

9 M. A. Chopra, *Fabrication Issues in the Development of Low Cost Flip Chip Plastic BGA Assemblies,* Proc. Surface Mount International, 1995, pp. 226-234.

10 R. Marrs, R. Molnar, B. Lynch, P. Mesher, and G. Olachea, *An Enhanced Performance low Cost BGA Package,* Proc. Surface Mount International, 1995, pp. 214-225.

11 G. B. Martin, M. S. Cole, P. J. Brofman, and L. S. Goldman, *The Effect of Substrate Thickness on CBGA Fatigue Life,* Proc. Surface Mount International, 1997, pp. 172177.
12 S. C. Bolton, A. J. Mawer, and E. Mammo, Influence of Plastic Ball Grid Array Design/Materials upon Solder Joint Reliability, *International Journal of Microcircuits and Electronic Packaging, Vol.* 18, No. 2, 1995, pp. 109-120.
13 A. R. Syed, *Significance of Design Parameters on the Thermal Fatigue Life of Plastic Ball Grid Array Packages,* ICEMCM '96 Proc., pp. 161-166.
14 R. Darveaux and A. Mawer, *Thermal and Power Cycling Limits of Plastic Ball Grid Array (PBGA) Assemblies,* Proc. Surface Mount International, 1995, pp. 315-326.
15 Y.-C. Cho and A. Mawer, Interconnect Reliability of a C4/CBGA at both Chip and Board Levels, *Journal of SMT,* April 1998, pp. 21- 27.
16 D. R. Banks, T. E. Burnette, R. D. Gerke, E. Mammo, and S. Mattay, Reliability Comparison of Two Metallurgies for Ceramic Ball Grid Array, *IEEE Trans. Components, Packaging, and Manufacturing Technology* - Part B, Vol. 18, No. 1, 1995, pp. 53-57.
17 D. R. Banks, T. E. Burnette, Y.-C. Cho, W. T. DeMarco, and A. J. Mawer, *The Effect of Solder Joint Voiding on Plastic Ball Grid Array Reliability,* Proc. Surface Mount Internatinal, 1996, pp. 121-126.
18 A. J. Mawer, S. C. Bolton, and E. Mammo, *Plastic BGA Solder Joint Reliability Considerations,* Proc. Surface Mount International, 1994, pp. 239-251.
19 S. Rooks, B. Benhabib, and K. C. Smith, *Development of an Inspection Process for Ball-Grid-Array Technology using Scanned-Beam X-Ray Lamingraphy,* Proc. Nepcon West, 1994, pp. 277-289.
20 A. Mawer, D. Cho and R. Darveaux, *The Effect of PBGA Solder Pad Geometry on Solder Joint Reliability,* Proc. Surface Mount International, 1996, pp. 127-135.
21 R. Rorgren, P.-E. Tegehall, and P. Carlsson, *Reliability of Ball Grid Array Packages in an Automotive Environment,* Proc. Surface Mount International, 1997, pp. 85-92.
22 R. Evans, M. Boulos, T. Huynh, V. Kane and W. Sanches, Implementation of Area Array, Chip Scale Packages, Ball Grid Arrays, and Ultra-Fine Pitch Devices, *Future Circuits International,* Vol. 2, Issue 1, 1997, pp. 51-55.
23 E. Bradley and K. Banerji, *Effect of PCB Finish on the Reliability and Wettability of Ball Grid Array Packages,* Proc. 45th Electronic Components & Technology Conf., 1995, 1028-1038.
24 V. F. Hribar, J. L. Bauer and T. P. O'Donnell, *Microstructure of Electroless NickelSolder Interactions,* Proc. of the 3rd International SAMPE Electronics Conference, 1989, pp. 1187-1199.
25 D. R. Frear, F. M. Hosking and P. T. Vianco, *Mechanical Behaviour of Solder Joint Interfacial Intermetallics,* Proc. of the Materials Development in Microelectronic Packaging Conference, 1991, pp. 229-240.
26 D. W. Finley, U. Ray, I. Artaki, P. Vianco, S. Shah, A. Reyes and M. Haq, *Assessment of Nickel-Palladium Finished Components for Surface Mount Assembly Applications,* Proc. Surface Mount International, 1995, pp. 941-953.
27 M. Walsh, Electroless Nickel Immersion Gold and Black Pad, *CircuiTree,* Vol. 14, No. 1, 2001, p. 10.
28 J. Lau, K. Gratalo, E. Schneider, T. Marcotte, and T. Baker, Solder Joint Reliability of Large Plastic Ball Grid Array Assemblies Under Bending, Twisting and Vibration Conditions, *Circuit World, Vol.* 22, No. 1, 1995, 27-32.
29 H. Quinones, M. Shatzkes, and J. Jaspal, *Reliability of Solder Ball Connection,* Proc. Surface Mount International, 1994, pp. 267-270

30 W. Engelmaier, BGA and CGA Solder Attachments: Results of Low-accelerated Reliability Test and Analysis, *Soldering & Surface Mount Technology,* No. 24, 1996, pp. 25-31.

31 K. Sturcken, Column Grid Array: High-Reliability Option for Packaging, *Advanced Packaging,* Aug. 2000, pp. 45-50.

32 A. Gallo and R Munamary, Popcorning: A Failure Mechanism in Plastic-Encapsulated Microcircuits, *IEEE Transactions on Reliability,* Vol. 44, No.3, 1995, pp. 362-367.

33 R. Munamarty, P. McCluskey, M. Pecht, and L. Yip, Popcorning in Fully Populated and Perimeter Plastic Ball Grid Array Packages, *Soldering & Surface Mount Technology,* No. 22, 1996, pp. 46-50.

34 F. Hua and B. Leong, *A Moisture Induced Failure in FCBGA Packages During Multiple Ref ow,* Proc. Surface Mount International, 1998, pp. 14-17.

35 A. Casasnovas and A. F. Moor, The Rational Use of Plastic Parts in Satellites, *EEE Links,* Vol. 4, No. 3, 1998, pp. 5-14.

36 K. T. Knadle and M. G. Ferril, *Failure of Thick Board Plated Through Vias with Multiple Assembly Cycles - The Hidden BGA Reliability Threat,* Proc. Surface Mount International, 1997, pp. 109-115.

37 A. Mawer, K. Simmons, T. Burnette, and B. Oyler, *Assembly and Interconnect Reliability of BGA Assembled onto Blind Micro and Through-Hole Drilled Via in Pad,* Proc. Surface Mount International, 1998, pp. 21-28.

38 C. Milkovich and L. Jimarez, *Ceramic Ball Grid Array Surface Mount Assembly and Rework,* Document APD-SBSC-101.0, IBM Corporation, 1998.

39 C. Milkovich and L. Jimarez, *Ceramic Column Grid Array Assembly and Rework,* Document APD-SCC-201.0, IBM Corporation, 1999.

40 G. Phelan and S. Wang, *Solder Ball Connection Reliability Model and Critical Parameter Optimization,* Proc. 43rd Electronic Components & Technology Conf, June 1993, pp. 858-862.

41 M. Wickham, C. Hunt, D. M. Adams, and B. D. Dunn, *An investigation into Ball Grid Array Inspection Techniques,* ESA STM-261, 1999, ESA Publication Division, Noordwijk, The Netherlands.

42 M. G. Pecht, R. Agarwal, and D. Quearry, Plastic Packaged Microcircuits: Quality, Reliability, and Cost Issues, *IEEE Trans. on Reliability, Vo.* 42, No. 4, 1993, pp. 513-517.

43 ESA PSS-01-738, *High-Reliability Soldering for Surface Mount and Mixed-Technology Printed-Circuit Boards,* Issue 1, ESA Publication Division, Noordwijk, The Netherlands, March 1991.

44 ESA PSS-01-710, *The Qualification and Procurement of Two-Sided Printed-Circuit Boards (Fused Tin-Lead or Gold-Plated Finish),* Issue 1, ESA Publication Division, Noordwijk, The Netherlands, October 1985.

45 M. Bevan, *Effect of Conformal Coating on the Reliability of LCCC Solder Joints Exposed to Thermal Cycling,* Proc. Surface Mount International, 1991, pp. 73 7-744.

46 H.-M. Tong, L. S. Mok, K. R. Grebe, H. L. Yeh, K. K. Srivastava and J. T. Coffin, Effects of Parylene Coating on the Thermal Fatigue Life of Solder Joints in Ceramic Packages, *IEEE Trans. Components, Hybrids and Manufacturing Technology, Vol.* 16, No. 5, 1993, pp. 571-576.

47 P. E. Kyle, *Non-Woven Aramid Reinforcements; Controlled Thermal Expansion Prepreg and Laminate for Printed Wiring Boards,* Proc. Nepcon West, 1995, pp. 24-32. 48

ECSS-Q-70-08A, *The manual soldering of high-reliability electrical connections,* ESA Publication Division, Noordwijk, The Netherlands, August 1999.

49 IPC-SM-785, *Guidelines for Accelerated Reliability Testing of Surface Mount Solder Attachments, IPC,* November 1992.

50 B. D. Dunn and P. Desplat, Evaluation of Conformal Coatings for Future Spacecraft Applications, ESA SP- 1173, ESA Publication Division, Noordwijk, The Netherlands, 1994.

51 R. D. Gerke, *Ceramic solder-grid-array interconnection reliability over a wide temperature range,* Proc. Nepcon West 94, 1994, pp. 1087-1094.

52 D. J. Lando, J. P. Mitchell and T. L. Welsher, *Conductive Anodic Filaments in Reinforced Polymeric Dielectrics: Formation and Prevention,* 17th Annual Proc. of Reliability Physics, pp. 51-63, 1979.

53 J. N. Lahti, R. H. Delaney and J. N. Hines, *The Characteristic Wearout Process in Epoxy-Glass Printed Circuits for High Density Electronic Packaging,* 17th Annual Proc. of Reliability Physics, pp. 39-43, 1979.

Annex A: Dye Penetrant Analysis of Soldered Grid Array Interconnections

Al Background

Dye penetrant inspection provides a way to detect discontinuities that are open to the surface of metallic items. Industry has incorporated dye penetrants to reveal defects such as cracks, delaminations and open seams. The traditional method is non-destructive, the liquid penetrant is applied to the dry metal surface being inspected, it enters the discontinuity aided by capillary forces and after a specified time the surface of the item is wiped clean and dried. The location of defects may be revealed by inspecting the surface for signs of dye which might seep out from the discontinuity. Black (ultraviolet) light will assist when the dye consists of a fluorescent liquid. Other liquids are often coloured with a red dye and can be highlighted when, after drying, the metal surface is covered (sprayed) with a white powder called a developer. This becomes stained by the dye and reveals the location of underlying defects.

The traditional use of dye penetrants for the inspection of soldered joints is not feasible because defective joints that contain cracks are usually covered by a rough surface caused by upsetting of the surface grain structure. Dye penetrant causes general staining of the solder and actual defects, such as thermal fatigue cracks, are impossible to distinguish from laps and orange peel effects on the solder fillet.

Destructive microsectioning methods are also used to investigate the depth of cracks that might occur within solder joints during environmental testing. Microsections are required as a final destructive test during the verification of surface mount technologies for space use [A1]. However, it is known that the plane of section can occasionally miss short cracks that have propagated in a different part of the joint. Whereas microsectioning is generally suitable for surface mount devices that have readily inspectable leads, it has only a limited use when applied to the evaluation of grid array packages where solder connections (balls or columns) are hidden from view and where the sheer numbers make microsectioning an almost impossible task.

"Destructive dye penetrant analysis" offers a three-dimensional view of cracks in solder joints to a component. The technique was originally developed by Motorola's Land Mobile Products Sector's Advanced Manufacturing Technology group [A2]. The component assembled on the printed circuit board was flooded with a dye penetrant liquid to define the cracked area. After having applied the dye, the component was removed by bending the board numerous times. The fractured solder joints were then visually inspected and photographs were made to record the position that dye had penetrated into the joint. This method works well if the cracks in the solder joints are large. If they are not large enough, the pads on the board will rip off from the laminate.

The method for dye penetrant analysis used in this investigation is described in this annex. It involves a development of the technique to remove the components that makes it possible to remove them even if the cracks in the solder joints are small.

A2 Application of Dye

In order to facilitate the application of the dye, a dam was created around the component using a modelling wax. A tape was applied to the via holes on the opposite side of the board to prevent the dye from escaping through them. The dam was then filled with the dye (Steel Red from DYKEM) and the board was placed in a vacuum chamber. Two evacuations were

made down to 100 mbar in order to remove any air trapped in the cracks. Since solvents in the dye evaporate during this process, it should be done as fast as possible to prevent the viscosity of the dye getting too high. The surplus dye was then poured out and the sample was dried at 100 °C for 15 minutes.

A3 Removal of Components

The upper side of the component package was roughened using a grinding paper and was then dried with a cloth wetted with acetone. A steel cylinder with a threaded hole was glued to the component using a two-part epoxy glue, Plastic Padding Super Steel from Loctite (Fig. Al). The steel cylinder had been shotblasted in order to improve the adhesion of the glue.

The board was then fixed by screws to an aluminium plate with a thickness of 1 cm. A hook was screwed to the steel cylinder and the sample was arranged so that a pulling force could be applied through the hook (Fig. A2). The whole arrangement was placed on a heating plate with the heat controlled by a thermocouple attached to the upper side of the board. The temperatures of the balls or columns were registered using another thermocouple.

A pulling force of 50 grams per joint was applied to the package (i.e. in total 31 kg to a 625 I/O BGA package). This force causes the solder to creep and the package can be removed without bending the board. If the solder joints are severely cracked, it may be possible to remove the package within a few hours at room temperature. However, in most cases it was necessary to heat the samples to be able to remove the packages within a reasonable time. By heating the solder joints to 140 °C, even packages with only small cracks in corner joints could be removed within one to two hours. However, the colour of the dye slightly faded at such high temperatures. Also, a good temperature control system is required to ensure that the temperature of the board will not rise above the melting point of the solder when the package becomes loose.

It should be noted that fading of the dye can be avoided by limiting the solder joint temperature to maximum 120 °C. This temperature of 120 °C was used to remove the packages in the main study of this report. The time required to remove the packages was, in most cases, less than two hours and at the most 8 hours.

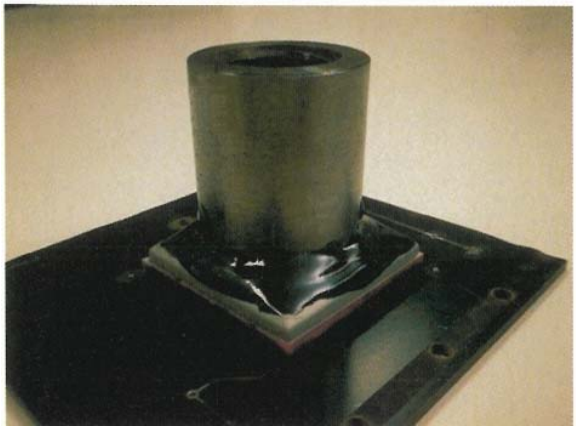

Figure A1. A component with a steel cylinder glued to it

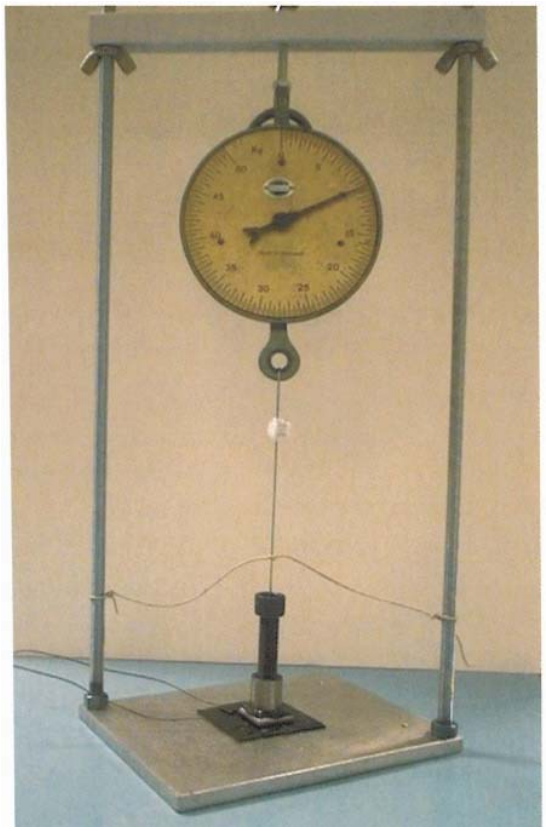

Figure A2. Arrangement, for applying a pulling force to a package

A4 Reference

A1 ESA PSS-01-738, *High-Reliability Soldering for Surface Mount and Mixed-Technology Printed-Circuit Boards,* Issue 1, ESA Publications Division, Noordwijk, The Netherlands, March 1991.

A2 S. C. Bolton, A. J. Mawer, E. Mammo, Influence of Plastic Ball Grid Array Design/Materials Upon Solder Joint Reliability, *International Journal of Microcircuits and Electronic Packaging, Vol.* 18, No. 2, 1995, pp. 109-120.

Annex B: Case Study of DBGA

B1 Background

The main part of this report describes experimental work related to the reliability of ceramic ball grid array and column grid arrays. These packages originated from IBM and had 625 I/Os, they were assembled, then environmentally tested and evaluated using methods that included destructive dye penetrant testing according to the procedure detailed in Annex A.

In order to gain further experience with the dye penetrant procedure, two additional grid array package terminations were evaluated. This Annex describes the analyses made on two Dimple BGA (DBGA) packages from Kyocera, which have 228 I/Os. These DBGAs had been assembled by a major European company according to well defined process procedures, using space-approved materials and cleaning methods. The assembled PCB had been verification tested by thermal cycling. The dye penetrant test results are as follows.

B2 Test Vehicle

The DBGA packages had a body size of 17 x 17 mm and 228 I/Os with a pitch of 1.0 mm. Both packages had daisy chain interconnections. The packages were soldered to a multilayer polyimide/glass board with tin-lead plated pads using vapour phase soldering. A flux was added to promote wetting but no additional solder. One package was soldered to a footprint with round solder pads (Component A) whereas the second package was soldered to a footprint having pads with a teardrop form (Component CX).

The test vehicle had been thermally cycled in air per ESA-PSS-01-738, but with the temperature extremes -55 to +125 °C. At 500 cycles the cycling was stopped. The package soldered to the footprint with round pads still functioned electrically after the thermal cycling test but one electrical defect had occurred in one row of I/Os on the other package.

B3 Dye Penetrant Analysis

The extent of cracking in the solder joints to the two DBGA packages was analysed using the procedure for dye penetrant analysis described in Annex A. The solder joints were heated to about 100 °C during the removal of the components. At this temperature, the components were removed within 30 min.

All solder balls remained on the printed circuit board for both packages. The fractures in the solder joints were very close to the component pads for all solder joints (Fig. B1). The majority of the solder joints were severely cracked for both components and to about the same extent (Fig. B2). The fractures in some corner solder joints were coloured completely red (Fig. B3). Thus, although failure had only been registered for Component CX, failure for Component A must have been imminent.

Figure B1. View of solder balls remaining on the PCB after removal of Component CX

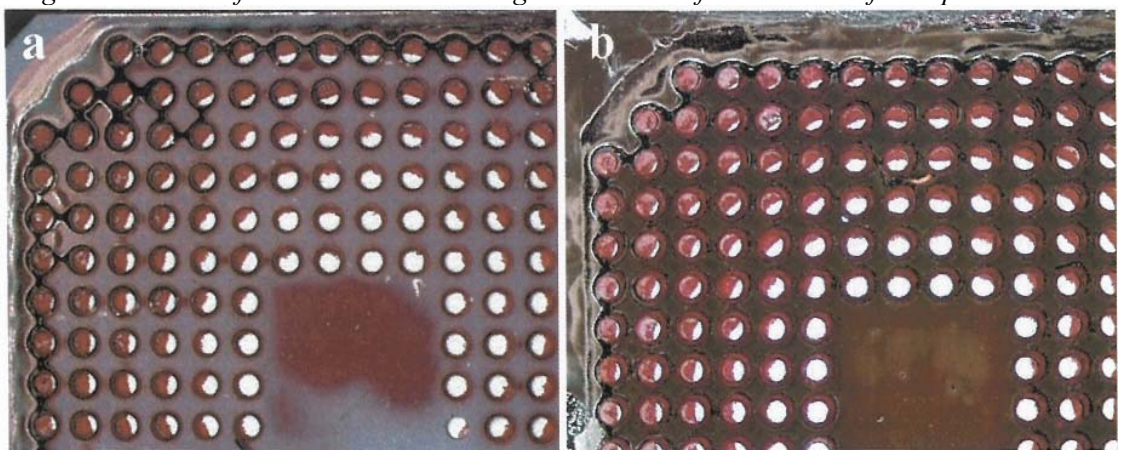

Figure B2. Extent of cracking in Component A (a) and to Component CX (b) analysed using dye penetrant

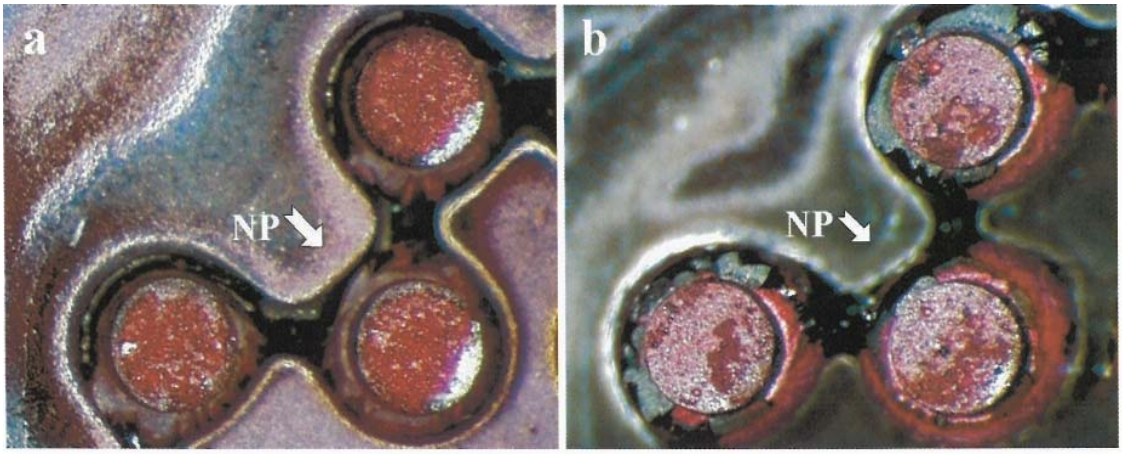

Figure B3. Close-up of the fracture to corner joints to Component A (a) and to Component CX (b)

The remaining solder balls on the PCB were broken away at some locations by deliberately gripping them with a micro-tweezer and pulling vertical to the board surface. This enabled us to examine the integrity of the joints towards the board pads. In all cases, the pads were ripped off from the laminate. For a connection in the inner row, no fracture in the laminate could be

observed (Fig. B4) whereas extensive cracking was observed for corner joints (Fig. B5). The cracks had formed on the inward side of the joints, as was also the case in the main study of this investigation. For one solder joint, the "inside" of the via-in-pad also was coloured red indicating damages to the copper plating in the via hole (Fig. B6). The results were similar for Component CX (Figs. B7-B9).

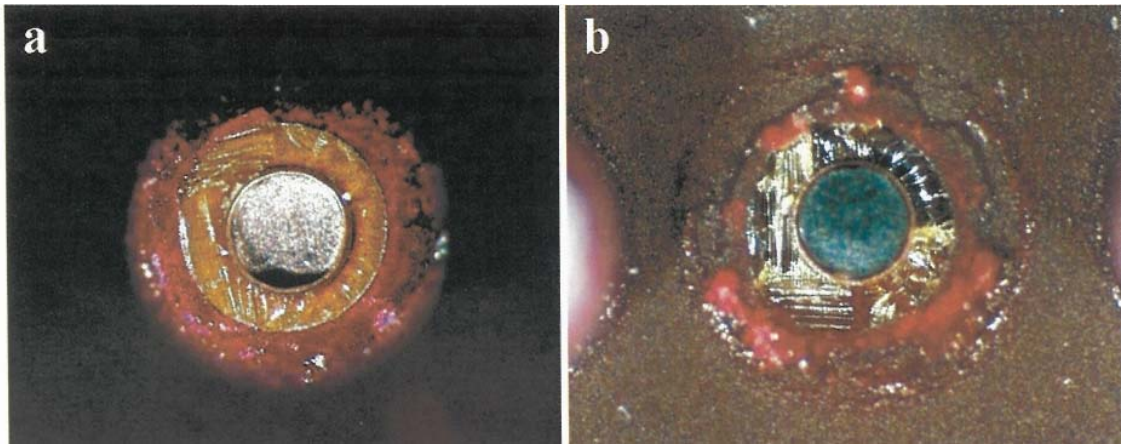

Figure B4. Views showing the fracture between a pad and the board laminate for a ball in the inner row to Component A. View (a) shows the ball with the underside of the ripped-off pad and view (b) shows the location on the PCB where the ball was attached

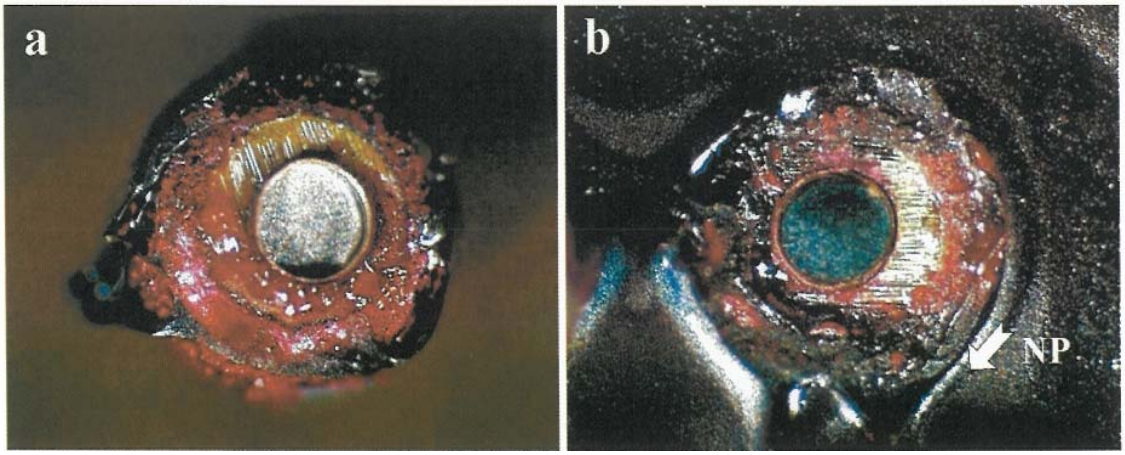

Figure B5. Views showing the fracture between a pad and the board laminate for a corner ball to Component A. View (a) shows the ball with the underside of the ripped off pad and view (b) shows the location on the PCB where the ball was attached

55

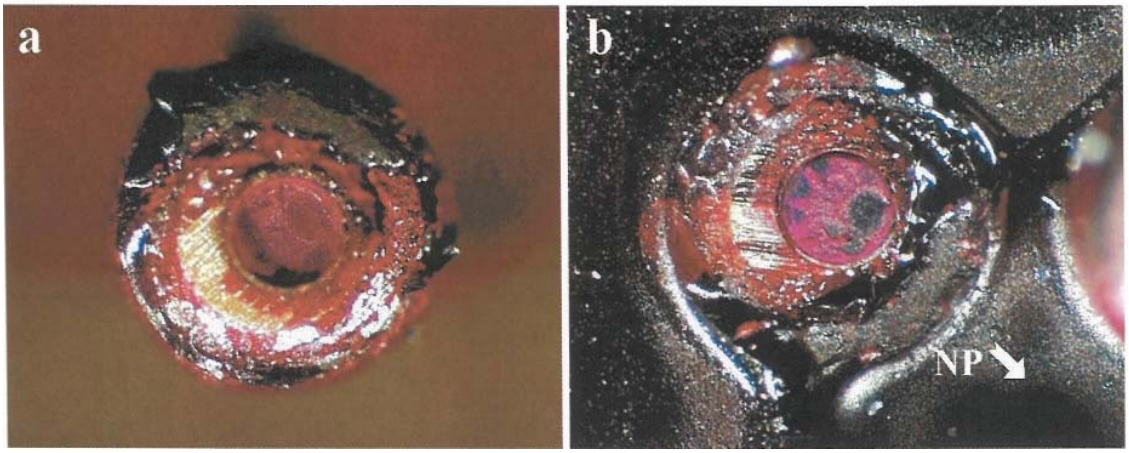

Figure B6. Views showing the fracture between a pad and the board laminate for a corner ball to Component A. View (a) shows the ball with the underside of the ripped off pad and view (b) shows the location on the PCB where the ball was attached

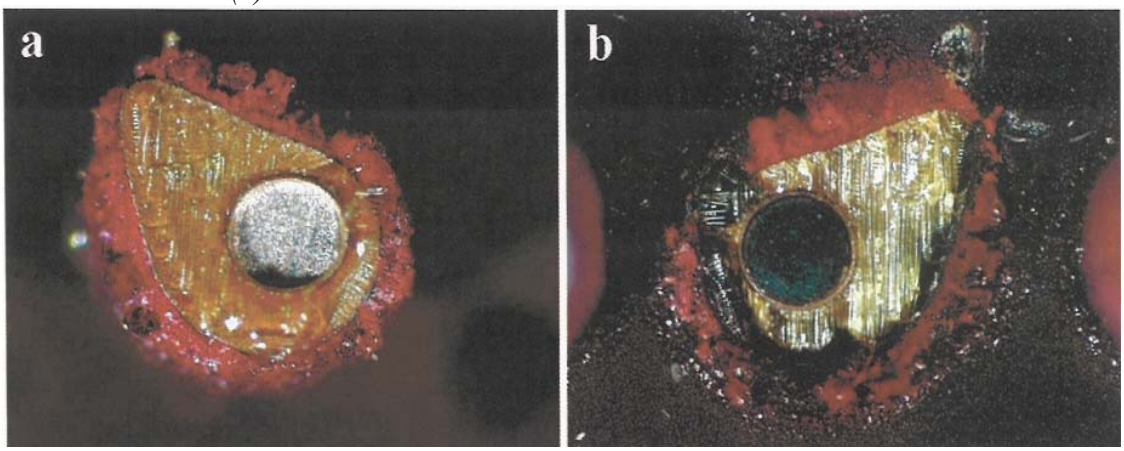

Figure B7. Views showing the fracture between a pad and the board laminate for a ball in the inner row to Component CX View (a) shows the ball with the underside of the ripped off pad and view (b) shows the location on the PCB where the ball was attached

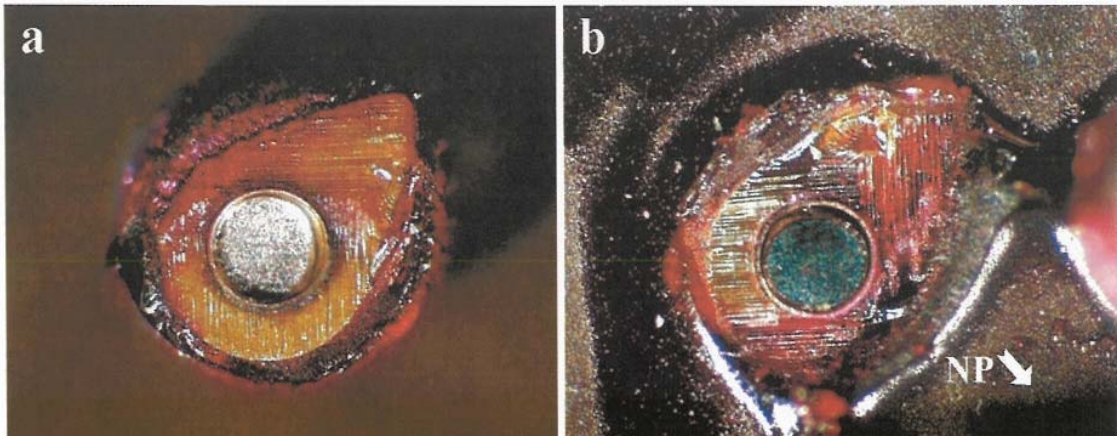

Figure B8. Views showing the fracture between a pad and the board laminate for a corner ball to Component A. View (a) shows the ball with the underside of the ripped off pad and view (b) shows the location on the PCB where the ball was attached

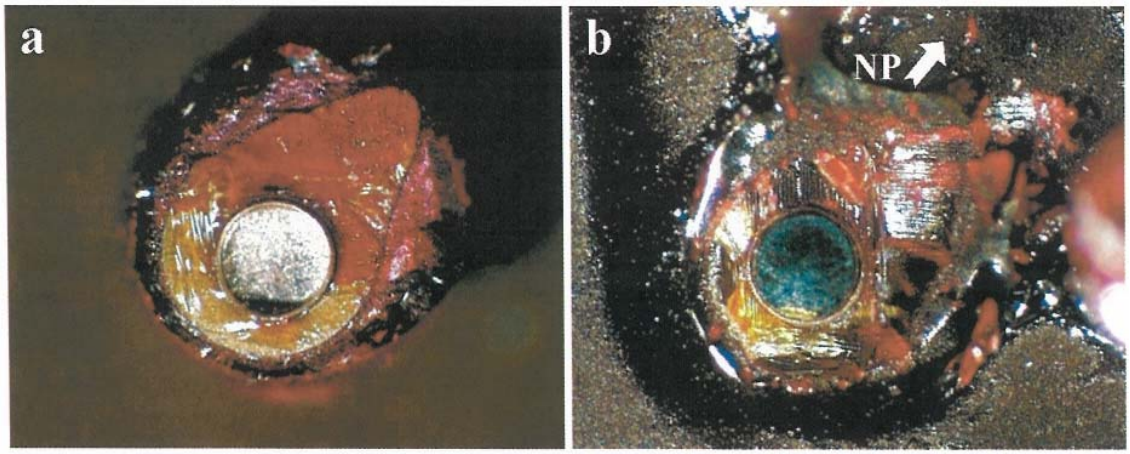

Figure B9. Views showing the fracture between a pad and the board laminate fbr a corner ball to Component A. View (a) shows the ball with the underside of the ripped off pad and view (b) shows the location on the PCB where the ball was attached